Extremely oligotrophic and complex organic compounds degrading microaerobic bacteria from Arabian Sea oxygen minimum zone sediments

Jagannath Sarkar[1,*], Mahamadul Mondal[1], Sabyasachi Bhattacharya[1,≠], Sumit Chatterjee[1], Nibendu Mondal[1,$], Subhajit Dutta[1], Saran N[1], Aditya Peketi[2], Aninda Mazumdar[2] and Wriddhiman Ghosh[1,*]

Author address:

[1] Department of Biological Sciences, Bose Institute, Kolkata - 700091, West Bengal, India

[2] Geological Oceanography, CSIR National Institute of Oceanography, Dona Paula, Goa - 403004, India

Present Address:

[≠] National Institute of Biomedical Genomics, Kalyani, West Bengal, India

[$] International Institute of Innovation and Technology, Kolkata, West Bengal, India

*** Correspondence:** wriman@jcbose.ac.in / jsarkarind@gmail.com

Key words: oxygen minimum zone sediments, aerobic bacteria, nitrate/nitrite reduction, complex organic compound degradation, fermentation, extreme oligotrophy

Running Title: Carbon cyclers from the sediments of a marine hypoxia

---

ABSTRACT

Sediments underlying marine hypoxias are huge sinks of unreacted complex organic matter, where despite acute O_2-limitation aerobic bacterial communities thrive, and near-complete depletion of organic carbon takes place within a few meters below the seafloor. However, little knowledge exists about how aerobic chemoorganotrophs survive in these sulfidic ecosystems, and what may be their potentials for degrading complex carbon compounds. To elucidate these questions, we isolated and characterized a number of aerobic bacterial chemoorganoheterotrophs from across a ~3-m sediment horizon underlying the perennial hypoxia of the eastern Arabian Sea. High levels of sequence correspondence between the isolates' genomes and the habitat's metagenomes and metatranscriptomes illustrated that the strains were widespread and active across the sediment cores explored. The isolates could catabolize several complex organic compounds of marine and terrestrial origins, via aerobic respiration at high as well as low O_2 concentrations. Some of them could also grow anaerobically on yeast extract or acetate by reducing nitrate and/or nitrite. Fermentation did not support growth in any of the strains, but enabled all of them to maintain a fraction of the cell population amidst prolonged anoxia. Under extreme oligotrophy, robust growth followed by

protracted stationary phase was observed for all the isolates at low cell density, irrespective of whether O_2 was high or low. While metabolic deceleration was apparently central to the strains' adaptation to dwindling organic carbon, O_2-limitation could be potentially surmounted via supplies from known producers of biogenic O_2, such as *Nitrosopumilus* species, which had copious footprints in the habitat's metagenomes.

INTRODUCTION

Marine sediments constitute one of the largest microbiomes on Earth (Hoshino et al. 2020), and act as the largest sink of organic carbon within the biosphere (Kallmeyer et al. 2012; Jørgensen et al. 2022; Ruben et al. 2023). Particularly within the shelf/slope territories of the continental margins, productivity in the oceanic water column, rate of sedimentation, and the extent of organic matter delivery to the seafloor are all very high, consequent to which O_2, followed by the less energy-efficient respiratory substrates such as nitrate, manganic, ferric, etc., get depleted within relatively shallow sediment depths (Canfield 1994; Seiter et al. 2005; Burdige 2007; Komada et al. 2016; Bhattacharya et al. 2021; Sarkar et al. 2022). This phenomenon is further accentuated in the mid-oceanic oxygen minimum zones (OMZs) that occur perennially along the western margins of the Earth's continents, and are considered to be the crucial bellwethers of ocean warming, deoxygenation, and acidification caused by global climate change (Wright et al. 2012; Long et al. 2021).

In the northwestern extension of the Indian Ocean a vast body of hypoxic water extends across the Arabian Sea and impinges upon a large shelve/slope area along the continental margins of India, Oman, Pakistan, Yemen, and Cape Guardafui in extreme north-eastern Somalia (Wyrtki 1971; Bange et al. 2005; Naqvi et al. 2006, Banse et al. 2014). This marine territory having dissolved O_2 concentration perennially below 20 μM is regarded as the thickest and largest of all the oxygen minimum zones (OMZs) of the global ocean (Acharya and Panigrahi 2016; Long et al. 2021). its upper boundary is positioned between 100 and 150 meters below the sea level (mbsl), the lower boundary between 1000 and 1200 mbsl, and the underlain benthic area (~230,440 km^2) constitutes more than a quarter of the Earth's total (~764,000 km^2) naturally-hypoxic seafloor (Helly and Levin 2004; Acharya and Panigrahi 2016). As the copious organic matter emanating from high microbial productivity in the euphotic zone descends down the water column, hectic biodegradation takes place, causing intense oxygen depletion and subsequent denitrification in the 100-1200 mbsl zone (Jayakumar et al. 2004; Lam and Kuypers 2011). However, due to hypoxia in the most part of

its travel path, a large fraction of the complex organic matter evades degradation while descending, and in doing so settles on the seafloor in its unreacted and labile form (Van Mooy et al. 2002; Cavan et al. 2017; Jessen et al. 2017). The deposition and degradation dynamics, i.e. the concentration, chemical nature, and fate of the organic matter that is delivered to the seafloor, determine the microbiome structure and function in the sediment system across the continental margin (Bhattacharya et al. 2021). With increasing water-depth (distance from the coast), lower sedimentation rate, so greater O_2-exposure time (irrespective of the O_2 concentration of the bottom-water) for the breakdown of the buried organic matter into simpler compounds, is encountered in the sediment surface (Canfield 1994; Kristensen et al. 1995; Burdige 2007; Middelburg 2019; Bhattacharya et al. 2021); consequently, down the sediment depths there is a core-wide intensification of the simple-fatty-acids-requiring anaerobic metabolisms of the carbon-sulfur cycle (Fernandes et al. 2018).

Whereas post-burial degradation of complex organic matter in the top-most strata of these sulfide-containing sediment systems is attributable to aerobic bacterial catabolism (Bhattacharya et al. 2021), it is remarkable that obligately aerobic bacteria are present and active (Bhattacharya et al. 2020), alongside sulfate-respiring anaerobes (Fernandes et al. 2018), across a ~3 meter sediment horizon of the Arabian Sea OMZ (ASOMZ), i.e. from the seafloor up to the depths where both organic carbon and sulfate are depleted and methane biogenesis begins (Fernandes et al. 2018). The presence of metabolically active and potentially growing aerobic bacterial communities up to the sulfate-methane transition zone is intriguing because there is little biochemical feasibility of O_2 production *in situ*, nor there exists any apparent chance of O_2 influx to the sediment system. That said, aerobic bacteria are known to thrive on nanomolar, or even lower, O_2 concentrations *in vitro* (Stolper et al. 2010), as well as in natural habitats (Ruff et al. 2023) including marine territories (Ulloa et al. 2012; Wright et al. 2012; Kalvelage et al. 2015; Garcia-Robledo et al. 2017) that are apparently anoxic. Whereas, “dark oxygen” produced by means of dismutation reactions is thought to provide potential sustenance to aerobic microbial communities in acutely O_2-limited ancient groundwater ecosystems (Ruff et al. 2023), minute spatiotemporal variations in the O_2 level of the chemical milieu has been hypothesized as the key driver of the stable co-occurrence of aerobic and anaerobic microorganisms in anoxic marine waters (Zakem et al. 2020). However, for the sedimentary realm of the ASOMZ, very little information is there about how the aerobic bacteria present could survive in this sulfidic habitat, and what could be their potentials for

degrading complex organic carbon that overfill the entire ecosystem and fuel hectic carbon-sulfur cycling *in situ* (Fernandes et al. 2018).

To address these questions the current study isolated and characterized aerobic bacterial chemoorganoheterotrophs from the sediment horizons underlying the heart of the ASOMZ, off the west coast of India. The strains isolated were investigated for their capabilities of growing under aerobic, micro-aerobic and anaerobic conditions, via degradation of polymeric carbohydrates, aromatic compounds, simple fatty acids, and also extremely low absolute concentrations of organic carbon. Population ecology, and *in situ* functionality, of the new isolates were assessed via whole genome sequence analysis, followed by investigations of genome-metagenome and genome-metatranscriptome correspondence. Furthermore, the microbiome structure of the habitat was examined in the light of the latest microbiological literature for potential secrets behind the sustenance of aerobic bacteria in these highly-reduced sediments; in doing so, plausible hypotheses were put forth for subsequent testing via fine-resolution explorations of analytical geochemistry and microbiology.

MATERIALS AND METHODS

Sample identity

Samples from the ~3 m long sediment cores SSK42/5 and SSK42/6 retrieved on board the research cruise RV *Sindhu Sankalp* 42 (SSK42) were used for the present studies of microbial ecology. The two cores, collected from 580 mbsl (latitude: 16°49.88' N, Longitude: 71°58.55' E) and 530 mbsl (latitude: 16°50.03' N, Longitude: 71°59.50' E) of the eastern Arabian Sea, across the western Indian margin, respectively, were investigated using culture-dependent as well as culture-independent methods at an average interval of 20 cm. For all the sediment depths explored along the two cores, sample replicates were collected for the investigation of pure culture isolates, metagenomes and/or metatranscriptomes, as described previously (Fernandes et al. 2018; Bhattacharya et al. 2020, 2021; Mandal et al. 2020).

Isolation of aerobic chemoorganoheterotrophs

Chemoorganoheterotrophic microbial strains were enriched and isolated in the presence of oxygen simultaneously from the bulk sediments of SSK42/5 and SSK42/6 via mixing of 1 g sample each from 0, 140 and 295 cmbsf for SSK42/5, and 2, 120 and 250 cmbsf for SSK42/6. For the bulk sample of each core, again, enrichment and isolation was carried out on three different culture media: (i) phosphate buffered artificial seawater (ASW, pH 7.5) medium

containing high concentration (0.5 g L^{-1}) of yeast extract as the energy and carbon source (this medium has been referred to as ASW_HY); (ii) ASW medium containing low concentration (0.001 g L^{-1}) of yeast extract as the energy and carbon source (this medium is referred to as ASW_LY here onward); and (iii) basal bicarbonate buffered (BBB, pH 7.5) medium containing sodium acetate (10 mM) as the energy and carbon source (this medium is referred to as BBB_A here onward).

Each liter of artificial seawater medium (ASW) contained 0.3 g $CaCl_2.2H_2O$, 0.5 g K_2HPO_4, 1.5 g $MgSO_4.7H_2O$, 25.1 g NaCl, 0.2 g $NaHCO_3$, 1 g $(NH_4)_2SO_4$, 2.4 g Tris, and 1 mL trace element solution. K_2HPO_4 was autoclaved separately and added to the medium. Each liter of the trace metals solution (pH 6.0) used in ASW comprised 1.61 g $CoCl_2.6H_2O$, 1.57 g $CuSO_4$, 50 g EDTA, 4.99 g $FeSO_4$, 5.06 g $MnCl_2$, 1.1 g $(NH_4)_6$ $MoO_{26}.4H_2O$ and 22 g $ZnSO_4.7H_2O$.

Each liter of basal bicarbonate buffered (BBB) medium contained 0.11 g $CaCl_2.2H_2O$, 0.41 g K_2HPO_4, 0.10 g $MgCl_2.6H_2O$, 0.3 g NaCl, 4 g $NaHCO_3$, 0.53 g $Na_2HPO_4.2H_2O$, 0.3 g NH_4Cl, 2 mL of the trace metal solution described above and 10 ml BME vitamin solution (Sigma-Aldrich).

Using the two core-specific bulk sediment samples and three different media types, overall six lines of enrichment and isolation were created. For each of these, 3 g of the relevant bulk sediment sample was added to 100 mL of the applicable culture medium contained in a 250 mL cotton-plugged Erlenmeyer flask having normal air in the headspace. The sediment-medium mixture was incubated aerobically for 24 hours at 15°C, following which the sediment was allowed to settle down and the supernatant was diluted serially and spread on agar plates of the same medium in which enrichment had taken place. These plates were incubated aerobically at 15°C, and from the biomass that appeared on them, pure culture strains were isolated after several rounds of dilution streaking. All the above steps of aerobic culture inoculation, transfer, and purification, plus those described subsequently, were carried out inside a Class II Biological Safety Cabinet (Esco, Singapore). Since all the new isolates could grow on ASW_HY, they were maintained in that medium. The strains were taxonomically classified up to the lowest possible category with the help of methods elaborated elsewhere (Saha et al. 2019); they were also deposited for public accession to the National Centre for Microbial Resource, National Centre for Cell Science, Pune, India.

Aerobic, microaerobic and anaerobic growth

For an aerobic growth experiment, a seed culture of the test strain was first generated by inoculating 20 ml ASW_HY broth with a loopful of inoculum from the working culture of the strain and then incubating the culture aerobically at 15°C. Cells were harvested from the exponentially growing seed culture, washed twice with and resuspended in 0.9% NaCl, and finally added to the experimental medium in such a way that the initial (0 h) cell density of the test culture came in the range of either 10^6 or 10^3 colony forming units (CFUs) mL^{-1}.

For an anaerobic or microaerobic growth experiment, seed culture preparation and test culture inoculation were carried out in the same way as above except for the fact that the washing of harvested cell pellets, as well as the inoculation of the test culture, was carried out within an H35 Hypoxystation (Don Whitley Scientific, UK), which was pre-set to 0 or 0.1% partial pressure of O_2 respectively (in either case humidity was maintained at 75%). Inside the H35, anaerobic condition (anoxia) was created via constant flow of N_2, CO_2 and H_2 at a volumetric ratio of 8:1:1, while microaerobic condition (hypoxia) was created by flowing N_2, CO_2 and O_2 at a volumetric ratio of 9:0.99:0.01. Furthermore, in case of an aerobic or microaerobic growth experiment the culture flask was cotton plugged, whereas for an anaerobic experiment, the culture bottle was screw-capped, and incubated inside the H35 Hypoxystation (in all the cases incubation temperature was 15°C). In this way, all aerobically grown cultures had 21% (v/v) O_2 in the head-space of the flasks, whereas microaerobic and anaerobic cultures had 0.1% (v/v) O_2, and zero partial pressure of O_2, in the head-space of the flasks, respectively.

So far as the culture media were concerned, those used for anaerobic growth experiments were supplemented with the following electron acceptors individually or collectively: $(CH_3)_3NO$ (27 mM), $(CH_3)_2SO$ (56 mM), Fe_2O_3 (125 mM), MnO_2 (1 mM), $NaNO_3$ (4 mM), $NaNO_2$ (4 mM), and Na_2SO_4 (10 mM); furthermore, separate anaerobic growth experiments were carried out by supplementing the media with 40 mM Fe_2O_3 and 17 g L^{-1} humic acid (Bhattacharya et al. 2020). Media used for anaerobic or microaerobic experiments contained thioglycolate (0.5 g L^{-1}) and resazurin (0.0001 g L^{-1}) for the purpose of deoxygenation, and subsequent monitoring of the O_2 level, respectively. Cultures exhibiting anaerobic growth via nitrate (NO_3^-) or nitrite (NO_2^-) reduction were measured for the concentration of these ions in the spent media by means of ion chromatography carried out using an Eco IC (Metrohm AG, Switzerland) furnished with a conductivity-based detector (Metrohm IC detector 1.850.9010). Separation of anions was carried out using the anion

exchange column Metrosep A Supp5 - 250/4.0 (Metrohm AG). The eluent comprised a mixture of $NaHCO_3$ (1.0 mM) and Na_2CO_3 (3.2 mM), while the regenerant encompassed sulfuric acid (100 mM); 100 µL of 100-fold diluted sample was injected in every chromatographic run, which in turn involved a flow rate of 0.7 mL min^{-1}. Chemicals standards provided by the platform manufacturer (Metrohm AG) were utilized to generate the calibration curves for the quantification of NO_3^- and NO_2^- ions; fluctuation range for each concentration measured was ±0.2 ppm.

Colony forming units (CFUs) present in a given experimental culture at any time-point of its incubation (this included the 0 h of incubation) was counted by taking 1 mL of the culture, diluting it by increasing logs of 10, then plating the different dilution grades in triplicates of ASW_HY agar, and finally counting the colonies appearing therein. In order to obtain the CFU count of 1 mL of the culture, colony counts recorded in the different dilution plates were multiplied by their respective dilution factors, following which the values were added up and averaged across the various dilution grades and replica plates generated. For aerobic growth experiments dilution plating was carried out inside the Biological Safety Cabinet, but in case of microaerobic and anaerobic growth, plating was carried out inside the H35 Hypoxystation; in all the three cases, incubation of the CFU-counting plates was carried out under aerobic condition.

Testing complex organic compound utilization

Isolates were tested for possible growth via catabolism of different complex organic compounds of marine and terrestrial origin, which in turn are considered to be relatively more amenable and recalcitrant towards degradation respectively (Cowie et al. 1992; Kristensen et al. 1995; Prahl et al. 1997; Aller and Blair 2004; Burdige 2007). Tested carbon compounds included agar, alginate, carrageenan and chitosan (in nature, these compounds are mostly of marine origin); cellulose, pectin and xylan (these originate mostly in terrestrial organisms); and benzoate and starch (these are produced by marine as well as terrestrial organisms). ASW medium was fortified with one of the abovementioned carbon compounds at a time (as a sole carbon source), and axenic cultures of each isolate were incubated individually in the nine different types of chemoorganoheterotrophic media formulated in the process. Agar (Type-I agar, Himedia, India) and carrageenan (Kappa-carrageenan, Merck, Germany), the two typical cell wall components of the red algae (Rhodophyceae), were added to ASW at the concentrations 2 g L^{-1} and 4 g L^{-1} respectively (Hosoda et al. 2003; Gobet et al. 2018).

Chitosan (Sigma-Aldrich, USA), a derivative of chitin found in the exoskeleton of shellfish, was provided at a concentration of 4 g L^{-1} (Gobet et al. 2018). Alginate (sodium salt of alginate, Himedia), found in the cell wall of marine macroalgae belonging to the family Phaeophyceae (brown algae), was added a concentration of 10 g L^{-1} (Jegatheesan et al. 2017). Cellulose (sodium salt of carboxymethylcellulose, Himedia), the main component of the cell wall of land plants, was provided at a concentration of 5 g L^{-1} (Olaniyi et al. 2019). Xylan (extracted from beechwood, Himedia), a major component of hemicellulose; and pectin (Himedia), a cell wall polysaccharide of terrestrial plants, were added at a concentration of 10 g L^{-1} each (Anand et al. 2010). Benzoate (sodium salt, Himedia) and water-soluble starch (Himedia) were added at the concentrations 5 mM (Moreno and Rojo 2008) and 4 g L^{-1} (Gobet et al. 2018) respectively.

Test of oligotrophy and fermentative abilities

ASW medium supplemented with extremely low concentration of yeast extract (1×10^{-12} g L^{-1}) as the energy and carbon source (ASW_ELY) was used to test the oligotrophic growth potentials of the new isolates, under aerobic, microaerobic, or anaerobic condition, starting with a bacterial density in the range of either 10^3 or 10^6 cells mL^{-1}.

Whether the isolates could grow or survive (maintain a fraction of the cell population in viable state) by means of fermentative metabolism was tested in ASW supplemented with pyruvate (5 g L^{-1} sodium pyruvate, Sisco Research Laboratories Pvt. Ltd., India) or glucose (10 g L^{-1} D-glucose, Merck, Germany), under anaerobic condition. Pyruvate, the end product of glycolysis, is an important intermediate of the central carbohydrate metabolism. It is the common substrate utilized by all fermentative bacteria: in some cases it supports growth under anaerobic condition (Cocaign-Bousquet et al. 1996; Wagner et al. 2005), while in others, including in a number of obligate aerobes, it helps preserve cell populations in the absence of O_2 (Eschbach et al. 2004; Pinchuk et al. 2011).

Phylogenetic and genomic characterization of the new isolates

Genomic DNA was prepared from the stationary-phase cultures of the new isolates using PureLink Genomic DNA Mini Kit (Thermo Fisher Scientific, USA). The 16S rRNA gene of each strain was amplified using PCR, and sequenced on a 3500xL Genetic Analyzer (Thermo Fisher Scientific), using the *Bacteria*-specific universal primers 27f and 1492r (Crocetti et al. 2000). The nearly complete 16S rRNA gene sequence of each strain was analyzed to identify its closest phylogenetic relative as described earlier (Ghosh et al. 2006; Mondal et al. 2022).

Whole genome shotgun sequencing was carried out separately for all the individual isolates using the Ion S5 (Thermo Fisher Scientific) and MinION (Oxford Nanopore Technologies, UK) next generation DNA sequencing technologies. Datasets of raw reads obtained using the two technologies were deposited in the Sequence Read Archive of National Center for Biotechnology Information (NCBI), USA, under the BioProject PRJNA309469, with accession numbers given in Table S4. For each genome, Ion S5 reads having Phred score above 20 and length above 100 nucleotides, and MinION reads having quality value greater than 10, were assembled together using Unicycler v0.5.0 in hybrid assembly format (Wick et al. 2017). The genomes were annotated using the Prokaryotic Genome Annotation Pipeline (PGAP) of NCBI which is located at https://www.ncbi.nlm.nih.gov/genome/annotation_prok/. The gene-catalog obtained from PGAP for each genome was functionally annotated further via search against eggNOG database v5.0 (Huerta-Cepas et al. 2019), using the online utility eggNOG-mapper v2.1.9 (Cantalapiedra et al. 2021). The annotated complete whole genome sequences obtained in this way were deposited in the NCBI GenBank, under the BioProject PRJNA309469, with accession numbers mentioned in Table S7 (the assembly statistics have also been presented in the same supplementary table). Furthermore, taxonomic identification of the isolated strains up to the lowest possible taxon was carried out on the basis of their genome-genome relatedness with closest phylogenetic relatives, determined in terms of digital DNA-DNA hybridization (dDDH) values, using Type Strain Genome Server (TYGS; Meier-Kolthoff and Göker 2019) of the Leibniz Institute DSMZ - German Collection of Microorganisms and Cell Cultures GmbH.

Metagenomics

The duplicate metagenomes taken out from the discrete sediment samples of SSK42/5 and SSK42/6 were individually sequenced, as described elsewhere (Bhattacharya et al. 2020; Mandal et al. 2020). Post merging of the dataset pair available for any given sediment sample, all reads having Phred score ≥20 and length ≥50 nucleotides were subjected to contig assembly experiments using Megahit v1.2.9 (Li et al. 2015). Genes or open reading frames (ORFs), followed by protein-coding sequences (CDSs), were detected and annotated within ≥100 nucleotide contigs using Prodigal v2.6.3 (Hyatt et al. 2010), and eggNOG-mapper v2.1.9 (Cantalapiedra et al. 2021) with the help of eggNOG database v5.0 (Huerta-Cepas et al. 2019), respectively.

To determine the level of genome-metagenome correspondence, all quality-filtered metagenomic reads (statistics given in Table S13) available for a given sediment sample were mapped onto the bacterial genome under consideration using Bowtie2 v2.4.5 in default mode (Langmead and Salzberg 2012).

Metatranscriptomics

Extraction of metatranscriptomes, removal of rRNAs, and 2 × 150 nucleotides paired-end sequencing by synthesis with dual indexing workflows on a HiSeq4000 platform (Illumina Inc., USA) were carried out as communicated previously (Bhattacharya et al. 2020, 2021; Mandal et al. 2020). For a given sediment sample, all metatranscriptomic reads having Phred score ≥20 were assembled (into contigs) using Megahit v1.2.9 (Li et al. 2015). Genes or ORFs, followed by CDSs, were delineated and annotated within ≥100 nucleotide contigs using Prodigal v2.6.3 (Hyatt et al. 2010), and eggNOG-mapper v2.1.9 (Cantalapiedra et al. 2021) with the help of eggNOG database v5.0 (Huerta-Cepas et al. 2019), respectively.

To determine the level of genome-metatranscriptome correspondence, all quality-filtered, mRNA-specific metatranscriptomic reads (statistics given in Table S15) available for a given sediment sample were mapped onto the bacterial genomes under consideration using Bowtie2 v2.4.5 in default mode (Langmead and Salzberg 2012). In order to remove potential rRNA-related reads that were there in the metatranscriptomic sequence datasets, the latter were searched with reference to the rRNA gene sequence database SILVA v138.1 (Quast et al. 2013), using the software Bowtie2 v2.4.5 in default mode.

Detection of *Nitrosopumilus*-specific 16S rRNA gene fragments within the metagenomic DNA samples

The *Nitrosopumilus*-specific primer pair N_pumi_420F (5'-TGTTGAATAAGGGGTGGGCA-3') and N_pumi_981R (5'-CCACCTCTCAGCTTGTCTGG-3'), obtained using the Primer-BLAST program available online (Ye et al. 2012), was first used to PCR amplify potential 16S rRNA gene fragments from the individual metagenomic DNA preparations available for the discrete sediment samples explored along SSK42/5 and SSK42/6. These PCR-products were expected to be approximately 560 bp long on the basis of the gene length bracketed by the two primers within the *Nitrosopumilus maritimus* genome. The 25 PCR-products obtained in this way were subsequently used as templates to perform nested PCR using the *Archaea*-specific primer pair A571F (5’-GCYTAAAGSRICCGTAGC-3’) and Ab909R (5’-TTTCAGYCTTGCGRCCGTAC-3’)

that amplify the V4-V5 overlapping region of all archaeal 16S rRNA genes (Baker et al. 2003). This helped eliminate all potential unspecific amplicons before the PCR-products were individually sequenced on an Ion S5 next generation DNA sequencer (Thermo Fisher Scientific, USA), as described earlier (Mondal et al. 2022). Reads contained in a given 16S rRNA gene sequence dataset were trimmed for their adapters, those having lengths <150 bp and Phred score <20 were filtered out, and then the remaining reads were annotated taxonomically using the online utility called RDP Classifier (Wang et al. 2007, Table S20).

Detection of nitric oxide dismutase genes within the assembled metagenomes of SSK42/5 and SSK42/6

Microbial dismutation of nitric oxide (NO) can be a potential source of O_2 within dark ecosystems (Ettwig et al. 2010; Kraft et al. 2022; Ruff et al. 2023). The NO dismutase (Nod) enzyme of bacteria such as *Candidatus* Methylomirabilis oxyfera, and strain HdN1, reportedly convert NO directly to N_2 and O_2 (Ettwig et al. 2010) whereas its homologs putatively present in ammonia (NH_3)-oxidizing archaea such as *N. maritimus* apparently carry out the same conversion via nitrous oxide (N_2O) formation (Kraft et al. 2022). To check whether there was any feasibility of NO-derived O_2 sustaining the aerobic bacteria of SSK42/5 and SSK42/6, every contig of each assembled metagenome obtained along the two sediment cores was used as a query sequence to search for genes encoding nitric oxide dismutase, using the blastx algorithm. For this purpose translated amino acid sequences of *nod* gene homologs from *Candidatus* Methylomirabilis oxyfera (NCBI accession numbers ANF28199.1, APP93282.1, ANF28196.1 and APP93283.1) were used as the subject database (notably, in public databases, no Nod sequence is available thus far from ammonia-oxidizing archaea). BLAST+ executables, a suite of command-line programs to run Basic Local Alignment Search Tool, available at the website of NCBI, was used for the aforesaid searches, and hits having more than 45 nucleotide alignment, less than 10^{-6} e value, and more than 40 percent identity were reported.

RESULTS

Aerobic chemoorganotrophs from ASOMZ sediments

Bacterial consortia were enriched from the bulk sediment samples of the two cores SSK42/5 and SSK42/6 via aerobic incubation in three distinct chemoorganoheterotrophic media, leading to the isolation of 39 pure culture strains (Table 1) that appeared to be distinct in terms of

colony morphology and texture. 30 of these were obtained on the copiotrophic ASW_HY medium that contained 0.5 g L^{-1} yeast extract as a source of complex organic carbon, 5 strains were obtained on the oligotrophic ASW_LY medium that contained low concentration (0.001 g L^{-1}) of yeast extract, and 4 were retrieved on the synthetic BBB_A medium that had acetate (10 mM) as the sole organic carbon source. 16S rRNA gene sequence-based taxonomic classification clustered the 39 isolates into nine species-level groups, which in turn were ascribable to eight genera: *Brevibacterium*, *Brucella*, *Gordonia*, *Halomonas*, *Halopseudomonas*, *Marinobacter*, *Mesobacillus* and *Stenotrophomonas*. Two species-level groups were found to represent two separate species of *Brevibacterium*; one representative isolate from each of the nine species-level clusters was chosen for downstream experiments (Table 1).

The representative isolate BDJS002 showed highest (98.6%) 16S rRNA gene sequence similarity with *Brevibacterium aurantiacum* NCDO 739, while its next closest relative *Brevibacterium antiquum* VKM Ac-2118 had 98.2% similarity. TYGS analysis identified BDJS002 as a potential novel species of *Brevibacterium* on the basis of ≤69.3% dDDH with the type strains of different *Brevibacterium* species.

Another representative isolate JSBI002 showed highest (99.8%) 16S rRNA gene sequence similarity with *Brevibacterium iodinum* DSM 20626, while the next closest relatives *Brevibacterium pigmentatum* MCCC 1A09842 and *Brevibacterium sediminis* CGMCC 1.15472 had 99.1% 16S rRNA gene sequence similarity each with JSBI002. TYGS analysis, however, identified the OMZ-sediment isolate as a potential novel species of *Brevibacterium* on the basis of 42.2% to 54.1% dDDH with the type strains of *B*. *sediminis*, *B*. *pigmentatum* and *B*. *iodinum*.

The representatives of the remaining seven species-level groups were classified under seven different genera. Isolate JSBI001 showed 100% 16S rRNA gene sequence similarity with *Brucella anthropi* NBRC 15819, *Brucella lupini* NBRC 102587 and *Brucella cytisi* ESC1, whereas TYGS-based genome analysis identified JSBI001 as closest to *B*. *anthropi* ATCC 49188, and thereby affiliated to the same species, on the basis of 76.4% dDDH value.

The OMZ-sediment isolate SMJS1 showed 100% 16S rRNA gene sequence similarity with *Gordonia hongkongensis* HKU50. TYGS corroborated SMJS1 as a member of *G. hongkongensis*, based on 78.4% dDDH with the latter's type strain.

Isolate BDJS001 exhibited highest (99.0%) 16S rRNA gene sequence similarity with *Halomonas sedimenti* QX-2, while the next closest relative *Halomonas glaciei* DD39 had

98.8% similarity. TYGS analysis identified BDJS001 as a potential novel species of *Halomonas* on the basis of ≤51.7% dDDH with the type strains of other closely related species of *Halomonas*.

Isolate SMJS2 exhibited highest (99.2%) 16S rRNA gene sequence similarity with *Halopseudomonas bauzanensis* BZ93. TYGS confirmed SMJS2 as a member of *H. bauzanensis* based on 86.7% dDDH with the latter's type strain.

The 16S rRNA gene of the OMZ-sediment isolate AN1 showed 100% sequence similarity with *Marinobacter segnicrescens* SS011B1-4, while strains of other *Marinobacter* species had ≤98.8% similarities. TYGS analysis also identified AN1 as a member of *M. segnicrescens*, on the basis of 87.1% dDDH with the latter's type strain.

Isolate SBJS01 had the highest (99.4%) 16S rRNA gene sequence similarity with *Mesobacillus jeotgali* YKJ-10, while strains of other *Mesobacillus* species exhibited 99.4% to 99.2% similarities. TYGS analysis designated SBJS01 as a potential novel species of *Mesobacillus* based on ≤32.1% dDDH with the type strains of different *Mesobacillus* species.

The 16S rRNA gene of the OMZ-sediment isolate SBJS02 possessed maximum (99.3%) sequence similarity with homologs from a number of *Stenotrophomonas* species, but TYGS analysis classified the OMZ-sediment strain as a member of *Stenotrophomonas maltophilia*, based on 78.7% dDDH with the latter's type strain.

Obligately aerobic nature of all but two new isolates

All the nine representative strains could grow aerobically [at 21% (v/v) O_2] in ASW_HY medium, with their CFU counts increasing to 0.6-3.9 × 10^4 percent of the corresponding initial levels, after 1-2 days of incubation (Fig. 1A, Table S1). They were therefore maintained routinely in ASW_HY under aerobic condition. All the new isolates could also grow aerobically in ASW supplemented with 10 mM sodium acetate (ASW_A), with CFU counts increasing to 0.5-1.7 × 10^4 percent of the corresponding initial levels, after 1-2 days of incubation (Table S1).

None of the ASOMZ-sediment isolates except *Brucella anthropi* JSBI001 could grow anaerobically [at zero partial pressure of O_2] in ASW_HY supplemented with $(CH_3)_3NO$, $(CH_3)_2SO$, Fe_2O_3, MnO_2, $NaNO_3$, $NaNO_2$, and Na_2SO_4. Cultures of the eight test strains belonging to the genera *Brevibacterium*, *Gordonia*, *Halomonas*, *Halopseudomonas*, *Marinobacter*, *Mesobacillus* and *Stenotrophomonas*, upon anaerobic incubation in ASW_HY supplemented with all the seven electron acceptors together, retained only 0.01-9.2 percent in their initial CFU counts after 4 days (Fig. 1C); no CFU was left in any of the eight cultures after

8 days (Table S1). On the other hand, after 12 days of incubation under these conditions, CFU count of *B*. *anthropi* JSBI001 increased to 8.3 × 10^4 percent of the initial (Fig. 1C, Table S1). After anaerobic incubation for 12 days in ASW_HY supplemented with $NaNO_3$, or $NaNO_2$, CFU count of JSBI001 increased to 1.1 × 10^4 percent, and 9.3 × 10^3 percent, of the initial values respectively (Table S1). Corroboratively, 3.9 mM $NaNO_3$ and 3.4 mM $NaNO_2$ were found to be depleted in the two cultures, as measured by ion chromatography of the spent medium. In contrast to the above data, individual supplementation of ASW with $(CH_3)_3NO$, $(CH_3)_2SO$, Fe_2O_3, MnO_2, or Na_2SO_4 caused the retention of no CFU in JSBI001 cultures after 8 days of anaerobic incubation (time-course data given in Table S1). Furthermore, none of the nine new isolates, including *B*. *anthropi* strain JSBI001, could render anaerobic growth (Fig. 1D) or maintain a fraction of the cell population in viable state (Table S1) in ASW_HY supplemented simultaneously with Fe_2O_3 and humic acids.

Subsequent to the above experiments, the new isolates were tested for their abilities to grow anaerobically in ASW_A medium. None of the OMZ-sediment isolates except *Halopseudomonas bauzanensis* SMJS2 could grow in the absence of O_2 when ASW_A was collectively supplemented with the electron acceptors $(CH_3)_3NO$, $(CH_3)_2SO$, Fe_2O_3, MnO_2, $NaNO_3$, $NaNO_2$, and Na_2SO_4. The eight test strains belonging to the genera *Brevibacterium*, *Brucella*, *Gordonia*, *Halomonas*, *Marinobacter*, *Mesobacillus* and *Stenotrophomonas*, when incubated in ASW_A supplemented with all the seven electron acceptors collectively, retained only 0.006-0.93 percent of their initial CFU counts after 4 days of incubation; no CFU was left in any of them after 8 days (Table S1). In contrast, the *H*. *bauzanensis* SMJS2 culture, after 12 days of incubation under these conditions, increased its CFU count to 2.1 × 10^4 percent of the initial level (Table S1). Furthermore, SMJS2, after anaerobic incubation for 12 days in ASW_A supplemented with $NaNO_2$, increased its CFU count to 2.0 × 10^4 percent of the initial value (Table S1); corroboratively, ion chromatography showed that 3.3 mM $NaNO_2$ was depleted in the SMJS2 culture. However, individual supplementation of ASW with $(CH_3)_3NO$, $(CH_3)_2SO$, Fe_2O_3, MnO_2, $NaNO_3$, or Na_2SO_4 caused the retention of no CFU in JSBI001 cultures after 8 days of anaerobic incubation (detailed data given in Table S1). Furthermore, none of the nine new isolates, including *H*. *bauzanensis* SMJS2, could render anaerobic growth or survival in ASW_A supplemented simultaneously with Fe_2O_3 and humic acids (Table S1).

Microaerobic growth and fermentative survival under anaerobic condition

Ability of the ASOMZ-sediment isolates to grow or survive under microaerobic condition [0.1% (v/v) O_2] was checked in ASW_HY medium. After incubation for 4 days under such conditions within the H35 Hypoxystation, CFU count of the test strains increased 0.7-3.7 × 10^3 percent (Table S1), while after 8 days the increase was found to be 0.3-2.0 × 10^4 percent for the different isolates (Fig. 1B and Table S1).

The ASOMZ-sediment isolates were tested for their potentials to grow or survive amid anoxia using fermentative metabolism. After anaerobic incubation for 4 days in ASW containing glucose or pyruvate, the strains retained 30.9% to 96.2%, and 66.7% to 89.5%, of their initial CFUs respectively (Fig. 1E and 1F); after 8 days, 15.2% to 54.7%, and 9.4% to 85.6% CFUs were retained respectively (Table S1). Notably, even after 64 days of anaerobic incubation in glucose or pyruvate supplemented ASW, CFU count of the culture did not come down to zero for any of the strains in question (Table S1). To confirm the role of glucose and pyruvate (as fermentative substrates) in the above survival process, anaerobic incubation was carried for all the nine strains in ASW only (i.e. without any energy and carbon source). After 8 days of anaerobic incubation in ASW, CFU count in the culture of all but one isolate came down to zero. The anaerobic ASW culture of *B. anthropi* JSBI001, despite retaining 1.2 × 10^3 CFUs mL^{-1} after 8 days, contained no CFU after 16 days of incubation (Table S1).

Growth on complex carbon compounds under aerobic and microaerobic conditions

The new isolates were tested for their abilities to grow aerobically, microaerobically, or anaerobically (Fig. 2 and Table S2), using agar, alginate, carrageenan, chitosan; cellulose, pectin, xylan; benzoate, or starch as the sole carbon source in ASW-based chemoorganoheterotrophic medium. Following are the results of aerobic incubation for 4 days.

(i) Agar was utilized by *Brevibacterium* sp. JSBI002, *B. anthropi* JSBI001, *Halomonas* sp. BDJS001, *Mesobacillus* sp. SBJS01 and *Stenotrophomonas maltophilia* SBJS02 for growth, with their CFU counts increasing to 0.04-1.6 × 10^4 percent of the respective initial levels.

(ii) Alginate was used by *Brevibacterium* sp. JSBI002, *B. anthropi* JSBI001, *Halomonas* sp. BDJS001, *Mesobacillus* sp. SBJS01 and *Gordonia hongkongensis* SMJS1 for growth; over the incubation, their CFU counts increased to 0.2-3.6 × 10^4 percent of the corresponding initial levels.

(iii) Carrageenan supported the growth of *Brevibacterium* sp. JSBI002, *B*. *anthropi* JSBI001, *Halomonas* sp. BDJS001, *Mesobacillus* sp. SBJS01 and *S*. *maltophilia* SBJS02, with the CFU counts of these bacteria increasing to 0.1-1.1 × 10^3 percent of the respective initial levels.

(iv) Chitosan supported the growth of *Brevibacterium* sp. JSBI002, *B*. *anthropi* JSBI001, *Mesobacillus* sp. SBJS01 and *S*. *maltophilia* SBJS02, with their CFU counts increasing to 0.3-1.4 × 10^3 percent of the corresponding initial levels.

(v) Cellulose supported the growth of only *Brevibacterium* sp. JSBI002, with the CFU count of the bacterium increasing to 1.9 × 10^2 percent of the initial.

(vi) Pectin supported the growth of *Brevibacterium* sp. BDJS002, *Brevibacterium* sp. JSBI002, *B*. *anthropi* JSBI001, *Halomonas* sp. BDJS001, *Marinobacter segnicrescens* AN1 and *S*. *maltophilia* SBJS02; over the incubation, the CFU counts of these bacteria increased to 0.1-1.4 × 10^4 percent of their initial levels.

(vii) Xylan did not support chemoorganoheterotrophic growth in any of the nine microorganisms tested (Fig. 2G);

(viii) Benzoate supported the growth of *Brevibacterium* sp. BDJS002, *Brevibacterium* sp. JSBI002, *B*. *anthropi* JSBI001, *Halomonas* sp. BDJS001, *G*. *hongkongensis* SMJS1 and *H*. *bauzanensis* SMJS2, with the CFU counts of these bacteria increasing to 0.06-3.2 × 10^4 percent of the respective initial levels.

(ix) Starch was utilized by *Brevibacterium* sp. JSBI002, *B*. *anthropi* JSBI001, *Halomonas* sp. BDJS001, *Mesobacillus* sp. SBJS01 and *S*. *maltophilia* SBJS02 for growth; over the incubation, the CFU counts of these organisms increased to 0.03-2.1 × 10^4 percent of their initial levels.

Following are the results of microaerobic incubation for 8 days.

(i) Agar was utilized by *Brevibacterium* sp. JSBI002, *B*. *anthropi* JSBI001, *Halomonas* sp. BDJS001 and *Mesobacillus* sp. SBJS01 for growth, with the CFU counts of these bacteria increasing to 0.9-2.4 × 10^3 percent of the respective initial levels.

(ii) Alginate was used for growth by *Brevibacterium* sp. JSBI002, *B*. *anthropi* JSBI001, *Halomonas* sp. BDJS001, *Mesobacillus* sp. SBJS01 and *G*. *hongkongensis* SMJS1, with the CFU counts of these bacteria increasing to 0.5-5.2 × 10^3 percent of their initial levels.

(iii) Carrageenan supported growth of *Brevibacterium* sp. JSBI002, *B*. *anthropi* JSBI001, *Halomonas* sp. BDJS001 and *Mesobacillus* sp. SBJS01, with the CFU counts increasing to 0.3-1.5 × 10^3 percent of the initial levels after the incubation.

(iv) Chitosan supported the growth of only *B. anthropi* JSBI001 and *Mesobacillus* sp. SBJS01, with the CFU counts of the two organisms increasing to 3.5×10^2 and 7.4×10^2 percent of their respective initial levels.

(v) Pectin was used by *Brevibacterium* sp. BDJS002, *Brevibacterium* sp. JSBI002, *B. anthropi* JSBI001, *Halomonas* sp. BDJS001, *M. segnicrescens* AN1 and *S. maltophilia* SBJS02 for growth; over the incubation, their CFU counts increased to $2.0\text{-}4.0 \times 10^2$ percent of the corresponding initial levels.

(vi) Cellulose, xylan, and benzoate did not support the growth of any of the nine microorganisms tested (Fig. 2E, G and H);

(vii) Starch was utilized by *Brevibacterium* sp. JSBI002, *Halomonas* sp. BDJS001 and *Mesobacillus* sp. SBJS01 for growth; over the incubation, the CFU counts of these bacteria increased to $0.7\text{-}2.3 \times 10^3$ percent of their initial levels.

After anaerobic incubation for 8 days, none of the test strains could use agar, alginate, carrageenan, chitosan; cellulose, pectin, xylan; benzoate, or starch as the sole carbon source to grow chemoorganoheterotrophically in ASW containing $(CH_3)_3NO$, $(CH_3)_2SO$, Fe_2O_3, MnO_2, $NaNO_3$, $NaNO_2$, and Na_2SO_4; or Fe_2O_3 and humic acids together (Fig. 2 and Table S2).

Extreme oligotrophy under aerobic and microaerobic conditions

The ASOMZ-sediment isolates were tested for their abilities to grow aerobically, microaerobically, or anaerobically, in ASW containing 1×10^{-12} g L^{-1} yeast extract. Irrespective of the oxygen concentration provided, no growth was observed in any of the nine test strains when the initial cell count of the culture was set at ~10^6 CFU mL^{-1} (Fig. 3A). In contrast, starting with an initial number of ~10^3 CFU mL^{-1}, the CFU counts of the different test strains increased to $0.06\text{-}1.3 \times 10^4$ percent or $0.5\text{-}6.7 \times 10^4$ percent of the corresponding initial levels, after 8 days of incubation, under aerobic or microaerobic condition respectively; subsequently, the CFU count remained static even after incubation for several weeks (Table S3). Low initial cell density, however, could not facilitate oligotrophic growth under anaerobic condition (Fig. 3B and Table S3).

Genome contents of the ASOMZ-sediment isolates

Annotation of the complete whole genome sequences of the nine new isolates showed that the strains possessed 3.6-5.3 megabase long, single circular chromosomes (Fig. 4; Table S7), in addition to which *B. anthropi* JSBI001 (pJSBI001, 88.9 kilobase long) and *H. bauzanensis*

SMJS2 (pSMJS2, 212.4 kilobase long) had one wild plasmid each, and *G*. *hongkongensis* SMJS1 had two such replicons, pSMJS1.1 and pSMJS1.2, that were 174.7 and 104.9 kilobase long, respectively (Fig. 5; Table S7).

While *G*. *hongkongensis* SMJS1 had the largest chromosome (and thereby the highest number of genes), *H*. *bauzanensis* SMJS2 had the smallest (this strain also had the lowest number of genes). Notwithstanding the wide discrepancy in the total gene content of their chromosomes, the ASOMZ-sediment strains exhibited more or less comparable patterns of CDS distribution across the various categories of clusters of orthologous genes (COG; Fig. 6; Table S7). In the chromosomes of all the nine ASOMZ-sediment strains >3% CDSs each were consigned to the COG categories (i) Amino acid transport and metabolism, (ii) Carbohydrate transport and metabolism, (iii) Cell wall structure and biogenesis of outer membrane, (iv) Coenzyme transport and metabolism, (v) Energy production and conversion, (vi) Inorganic ion transport and metabolism, (vii) Lipid transport and metabolism, (viii) Molecular chaperones and related function, (ix) Signal transduction, (x) Transcription, and (xi) Translation, ribosomal structure and biogenesis. Five out of the nine strains, namely *Brevibacterium* sp. JSBI002, *B*. *anthropi* JSBI001, *Halomonas* sp. BDJS001, *M*. *segnicrescens* AN1 and *Mesobacillus* sp. SBJS01, had maximum CDSs ascribed to the COG category Amino acid transport and metabolism. Whereas three strains, *Brevibacterium* sp. BDJS002, *G*. *hongkongensis* SMJS1 and *S*. *maltophilia* SBJS02 had maximum number of their CDSs attributed to Transcription, *H*. *bauzanensis* SMJS2 had most CDSs affiliated to the category Cell wall structure and biogenesis of outer membrane.

For most of the COG categories, more or less equivalent percentages of CDSs were allocated in the different genomes. However, relatively higher proportions of CDSs were attributed to Cell division and chromosome partitioning in *Mesobacillus* sp. SBJS01; Carbohydrate transport and metabolism in *Brevibacterium* strains BDJS002 and JSBI002, *B*. *anthropi* JSBI001, and *Halomonas* sp. BDJS001; Energy production and conversion in *H*. *bauzanensis* SMJS2; Lipid transport and metabolism in *G*. *hongkongensis* SMJS1, compared with the other ASOMZ-sediment isolates.

pSMJS2 of *H*. *bauzanensis* SMJS2 was the largest of the four plasmids identified across three of the nine ASOMZ-sediment isolates; it also contained a higher number of CDSs (275) than the other three plasmids (Table S7). In contrast, pJSBI001 of *B*. *anthropi* JSBI001 was the smallest of the four plasmids detected in terms of size as well as gene content (109 CDSs encompassed in all). In the plasmid bearing isolates, for most of the COG categories,

comparable percentages of CDSs were allocated in the genome and the plasmid(s). However, as a consistent trend, (i) Defense mechanisms; (ii) Mobilome: prophages, transposons; and (iii) Replication, recombination and repair, had higher percentages of plasmid-borne genes allocated, compared with what percentages of chromosome-borne genes were attributed to these COG categories (Fig. 6; Table S7). Furthermore, the four plasmids also differed among themselves in terms of the proportions of CDSs allocated under a number of COG categories. For instance, relatively higher proportions of CDSs were allocated to (i) Carbohydrate transport and metabolism, (ii) Cell division and chromosome partitioning, (iii) Cell wall structure and biogenesis of outer membrane, and (iv) Lipid transport and metabolism in pSMJS1.2; (i) Amino acid transport and metabolism, (ii) Inorganic ion transport and metabolism, and (iii) Replication, recombination and repair, in pJSBI001; (i) Defense mechanisms (ii) Mobilome: prophages, transposons, and (iii) Replication, recombination and repair in pSMJS1.1; and (i) Signal transduction in pSMJS2, compared with the other plasmids identified.

The overall similarities and dissimilarities of the chromosomes and plasmids of the new isolates were holistically and quantitatively illustrated in a dendogram that clustered the replicons based on their gene contents across COG categories (Fig. 6). Here, the chromosomes of *M*. *segnicrescens* AN1, *H*. *bauzanensis* SMJS2, *S*. *maltophilia* SBJS02, and *Mesobacillus* sp. SBJS01 formed a distinct cluster, while those of *Halomonas* sp. BDJS001, *B*. *anthropi* JSBI001, *Brevibacterium* sp. JSBI002, *Brevibacterium* sp. BDJS002, and *G*. *hongkongensis* SMJS1 formed another divergent branch. Whereas the plasmids pSMJS1.1 and pSMJS1.2 of *G*. *hongkongensis* SMJS1, together with pSMJS2 of *H. bauzanensis* SMJS2, occupied a clearly distinct branch of the dendogram, the plasmid pJSBI001 harbored by *B. anthropi* JSBI001 branched intermediately between the two major clusters harboring the chromosomes and the plasmids.

Genes conferring bioenergetic versatility to the ASOMZ-sediment strains

Genome analysis revealed the presence of low as well as high O_2-affinity cytochrome oxidases in all the nine strains isolated from ASOMZ sediments. Genes for *aa3*-type cytochrome oxidase (*COX10*, *ctaB*, *cyoE* and *COX15*) and cytochrome-*bd* ubiquinol oxidase (*cydAB*) were detected in all the nine isolates, while those for *cbb3*-type cytochrome oxidase (*ccoNOPQ*) were identified in *B*. *anthropi* JSBI001, *Halomonas* sp. BDJS001, *H*. *bauzanensis* SMJS2 and *M. segnicrescens* AN1 (Table S8).

B. *anthropi* JSBI001, the only isolate capable of anaerobic growth via nitrate and nitrite respiration, was found to contain all genes that are required for complete denitrification (reduction of nitrate to dinitrogen); these included *narGHI* for nitrate reductase, *nirK* for nitrite reductase, *norBC* for nitric oxide reductase, and *nosZ* for nitrous oxide reductase. The *H*. *bauzanensis* strain SMJS2, which could perform anaerobic growth via nitrite respiration alone, contained all the genes needed for the reduction of nitrite to dinitrogen; these included *nirS* for nitrite reductase, *norBC* for nitric oxide reductase and *nosZ* for nitrous oxide reductase. The SMJS2 genome also encompassed a nitrite reductase (*nirBD*) homolog for the dissimilatory reduction of NO_2^- to NH_3.

Although none of the other ASOMZ-sediment isolates exhibited nitrate or nitrite respiration in ASW_HY and ASW_A, three of them possessed genes for the dissimilatory reduction of nitrate and/or nitrite. The genome of *Halomonas* sp. BDJS01 contained all the oxidoreductase genes that are required to reduce NO_3^- to NH_3; these included *narGHI* for nitrate reductase, and *nirBD* for nitrite reductase. The *M*. *segnicrescens* AN1 genome encoded all the enzymes required for the reduction of NO_2^- to N_2O; these included the NirS nitrite reductase, and the NorBC nitric oxide reductase. The AN1 genome also encoded the enzyme needed for the reduction of NO_2^- to NH_3, namely the NirBD nitrite reductase. *Mesobacillus* sp. SBJS01 encoded two distinct enzyme systems for NO_2^- reduction to NH_3; these included the nitrite reductases NirBD and NrfAH. The genomes of *Brevibacterium* strains BDJS002 and JSBI002, *G*. *hongkongensis* SMJS1, and *S*. *maltophilia* SBJS02 encoded no dissimilatory nitrate/nitrite reductase (Table S9).

Genes such as *pta* encoding phosphate acetyltransferase, *ackA* encoding acetate kinase, and *ldhA* coding for lactate dehydrogenase were detected in the genomes of all the new isolates except *Brevibacterium* sp. BDJS002, *G*. *hongkongensis* SMJS1 and *S*. *maltophilia* SBJS02 (Fig. 7, Table S9); all these enzymes are known to be central to fermentative metabolism and energy generation under anaerobic condition.

Genes for complex organic matter degradation in the new isolates

All the new isolates were found to have multiple genes for enzymes that can break the different glycosidic bonds of diverse polyglucan and polygalactan compounds (Fig. 7, Table S10). These glycosidic hydrolases could be instrumental in the organisms' degradation of, and growth on, diverse homo- and hetero-polysaccharides of glucose, galactose, xylose, and/or its derivatives (Fig. 2).

- *Brevibacterium* sp. BDJS002 and JSBI002 encoded five glycoside hydrolases each: of these, three each acts on linkages present in polyglucan, one each on polygalactans linkages, and one is unspecified in terms of its putative function.
- *B*. *anthropi* JSBI001 coded for 10 glycoside hydrolase homologs: four of these putatively act on polyglucan linkages, two on polygalactan linkages, three on peptidoglycans, while one is functionally unspecified.
- *G*. *hongkongensis* SMJS1 encoded 15 glycoside hydrolases, with 13 putatively acting on polyglucan linkages and two on linkages between polygalactans.
- *Halomonas* sp. BDJS001 encoded four glycoside hydrolases, with two putatively acting on polygalactan linkages, and one each on polyglucans and peptidoglycans.
- *H*. *bauzanensis* SMJS2 encoded four glycoside hydrolases, all of which putatively act on linkages between polyglucans.
- *M. segnicrescens* AN1 coded for one glycoside hydrolase, which putatively acts on polygalactans.
- *Mesobacillus* sp. SBJS01 encoded 19 glycoside hydrolases, of which 13 putatively act on oligo-/poly-glucans, three act on polygalactans, and three are functionally unspecified.
- *S*. *maltophilia* SBJS02 encoded 16 glycoside hydrolases of which 14 putatively act on linkages between polyglucans, one on polygalactans, and one has putative lysozyme activity.

In contrast to the widespread of genes for glycosidic hydrolases, enzymes governing the catabolic transformation of benzoate to catechol were found to be encoded by the genomes of only three out of the nine OMZ-sediment strains, namely *G*. *hongkongensis* SMJS1, *Halomonas* sp. BDJS001 and *H*. *bauzanensis* SMJS2 (Fig. 7, Table S11).

Genomic bases of cell density dependent oligotrophy in the isolates

Genes coding for proteins concerned with signal transduction in response to carbon starvation were found to be present in all the nine isolates (Table S12). While *Brevibacterium* sp. BDJS002 encoded one homolog each of the carbon starvation gene *cstA* and the *relA* mediator of stringent response to nutrient-level fluctuation, JSBI002 contained three *cstA* and one *relA* loci. The genome of *B*. *anthropi* JSBI001 encompassed two loci encoding the stringent starvation protein B (*sspB*), and one locus for the stringent response mediator *spoT*. *G*. *hongkongensis* SMJS1 contained a *relA* gene only, while *Halomonas* sp. BDJS001 contained one homolog each for *sspA*, *sspB* and *relA*, and *H*. *bauzanensis* SMJS2 encoded a

cstA, *sspA*, *sspB*, *relA* and *spoT* gene each. Whereas *M. segnicrescens* AN1 encoded one copy each for *sspB*, *relA* and *spoT*, *Mesobacillus* sp. SBJS01 coded for a *cstA* and a *relA* gene. *S*. *maltophilia* SBJS02 encoded one *CstA*, *relA*, *sspA*, *sspB*, and *spoT* gene each.

All the nine genomes analyzed encompassed a large number of genes for quorum sensing, including those attributed to the Lux regulon (Table S12). *Brevibacterium* sp. BDJS002 and JSBI002 encoded 16 and 11 Lux homologs respectively, while *B*. *anthropi* JSBI001 also encompassed 11 such genes. In contrast, *Halomonas* sp. BDJS001 encoded four Lux genes, whereas *M. segnicrescens* AN1 and *Mesobacillus* sp. SBJS01 encompassed two and five respectively. The genomes of *S*. *maltophilia* SBJS02 and *G*. *hongkongensis* SMJS1 coded for nine and 20 Lux genes respectively. In addition to the Lux regulon constituents, the genomes of *Halomonas* sp. BDJS001, *H*. *bauzanensis* SMJS2, *M. segnicrescens* AN1, *Mesobacillus* sp. SBJS01 and *S*. *maltophilia* SBJS02 were found to encode the alternative sigma factor RpoE.

The chemoorganotrophic strains are ubiquitous and active across the sediment horizon explored

When quality-filtered reads from the datasets of metagenomic sequence available for the 25 discrete sediment samples investigated across SSK42/5 and SSK42/6 (Table S13) were mapped individually onto a database comprising the genomes of the nine isolates, sizeable percentages of reads from all the metagenomic datasets mapped onto each of the genomes constituting the target (subject) database (Table S14). As an exception, only for the metagenome of the 190 cmbsf sample of SSK42/5 no read mapped on to the *Brevibacterium* strains BDJS002 and JSBI002. Collectively, the nine chemoorganoheterotrophs accounted for approximately 0.1% to 1.3% of the metagenomes analyzed along SSK42/5, and 0.5% to 11.3% of those analyzed along SSK42/6. In SSK42/5, cumulative abundance of these organisms remained largely consistent (range-bound between 0.1% and 0.3% of a metagenome) from the core-top till the core-bottom, except for two spikes at 45 and 90 cmbsf where these strains accounted for 1.3% and 1.1% of the metagenome (Table S14). In SSK42/6, however, overall representation of these organisms in the metagenome decreased from the core-top until 135 cmbsf (from 2.3% to 0.5% of the metagenome), then increased (up to 11.3%) until 250 cmbsf, and eventually decreased again to 1.1% at 275 cmbsf sediment depth (Table 14). With regard to the individual isolates, maximum percentage of reads mapped on to the genome of *M*. *segnicrescens* AN1, in case of almost all the metagenomes (24 out of

the total 25) analyzed across the two cores; only for 275 cmbsf of SSK42/6, most reads mapped on to the genome of *Halomonas* sp. BDJS001 (Table S14).

When quality-filtered, mRNA-specific reads from the metatranscriptomic sequence datasets obtained for the surface and subsurface sediments of SSK42/5 (0 and 15 cmbsf) and SSK42/6 (2 and 15 cmbsf) were mapped separately onto the database comprising the genomes of the new isolates, considerable proportions of reads from all the four metatranscriptomic datasets mapped onto each of the genomes (Table S16). Collectively, the genomes of the nine isolates accounted for approximately 16.6% and 9.7% of the 0 cmbsf and 15 cmbsf metatranscriptomes of SSK42/5, and 19.8% and 8.9% of the 2 cmbsf and 15 cmbsf of SSK42/6. Concurrently, in the same surface to subsurface trajectory, most of the individual genomes also exhibited decrease in their representation in the metatranscriptomic dataset (Table S16). Subsequently, to check what proportion of the metabolically active sedimentary community near a core-bottom comprised the new isolates, reads from the metatranscriptomic dataset available for the sediment sample from 275 cmbsf of SSK42/6 were mapped onto the genomes of the new isolates. Collectively, the nine genomes accounted for approximately 20.7% of this metatranscriptome. As for the individual isolates, maximum percentage of reads mapped on to the genome of *M*. *segnicrescens* AN1, in case of all the five metatranscriptomes analyzed (Table S16).

In situ expression of metabolisms that characterized the ASOMZ-sediment isolates

The quality-filtered metatranscriptomic datasets available for the two surface-sediment samples (0 and 2 cmbsf for SSK42/5 and SSK42/6 respectively), two subsurface sediment samples (15 cmbsf for both the core), and one deep-sediment sample (275 cmbsf from SSK42/6), were assembled *de novo* individually, and then the contigs obtained were annotated for putative CDSs. The five CDS-catalogs obtained in this way were then searched for homologs of the genes that generally govern those metabolic properties which were identified above as central to the ecological fitness of the chemoorganotrophic isolates. ≥99.2% reads from each of the five individual metatranscriptomic datasets contributed to the corresponding assemblies, which in turn yielded 4491–11954 contigs, at 188X–1120X average coverages. For the different assemblies, maximum and average contig lengths ranged between 13772–616923, and 453–4258, nucleotides respectively. Length of the consensus sequences obtained from the five assemblies ranged between 3.7 and 22.4 mb. The assembled

metatranscriptomes encompassed 9254–28806 ORFs, of which 6589–24073 were identified as putative CDSs (Table S15).

Different genes governing the breakdown of complex carbon compounds, including those encoding glycoside hydrolases, and aromatic compounds degradation (mineralization) enzymes, were identified in all the five assembled metatranscriptomes. Considerable number of genes for quorum sensing (Lux regulon), oligotrophy (starvation endurance genes such as *sspA*, *sspB*, *cstA* and *cstB*), aerobic respiration under acutely hypoxic condition (high O_2-affinity *cbb3*-type cytochrome oxidase and cytochrome-*bd* ubiquinol oxidase), and survival by fermentative energy transduction (genes such as *ldhA*, *ackA* and *pta*, the protein products of which can generate ATP from carbon substrates in the absence of O_2) were also detectable within each of the five metatranscriptomes assembled (Table S17).

Molecular signatures of *Nitrosopumilus* and nitric oxide dismutase in the metagenomes of SSK42/5 and SSK42/6

After merging the duplicate metagenomic sequence datasets available for the discrete sediment samples of SSK42/5 and SSK42/6, 1.8-12.6 million reads were obtained for each sample (Table S13). Quality filtration of each merged dataset for ≥50 nucleotides length and ≥20 Phred score retained 1.3-11.0 million reads for the different samples. *De novo* assembly of the individual, merged and quality-filtered, metagenomic read-sets yielded 56826–994006 contigs, with 60% to 94% of the reads from the different sets participating in the corresponding assemblies at 6X to 20X average coverages. For the different assemblies, maximum and average contig lengths ranged between 29237–280321 nucleotides and 239–581 nucleotides respectively. Length of the consensus sequences obtained from the five assemblies ranged between 23.2 and 258.4 mb. The assembled metagenomes individually encompassed 70133–997128 complete or partial ORFs, of which again 34347–278069 could be annotated functionally as putative CDSs (Table S13). When the 25 gene-catalogs obtained in this way were searched for CDSs having maximum sequence similarities with homologs from species of *Nitrosopumilus*, 0.01-0.19% of the CDSs annotated for the 12 discrete samples of SSK42/5 were ascribable to *N. maritimus* and 0.01-0.22% to *Nitrosopumilus sediminis* (Fig. 8 and Table S18). Likewise, 0-0.09% of the CDSs annotated for the 13 sediment samples of SSK42/6 were ascribable to *N. maritimus* (the only sediment site to have no *N. maritimus* affiliated CDS was 250 cmbsf of SSK42/6) and 0.01-0.11% to *N. sediminis* (Fig. 8 and Table S19).

Assembled metagenomes of all the sediment samples of SSK42/5 and SSK42/6, except those of 220 and 265 cmbsf of the latter core were found to encompass genes encoding nitric oxide dismutase (Nod). In SSK42/5, most numbers of CDSs – 19, 17, and 10 – for Nod were detected in 160 cmbsf, 190 cmbsf, and 0 cmbsf, respectively. In SSK42/6, most CDSs – 17, 14, 11, 11, and 10 – for Nod were detected in 2 cmbsf, 120 cmbsf, 60 cmbsf, 75 cmbsf, and 90 cmbsf, respectively (Table S20).

Furthermore, the metagenomic DNA preparations available for the 25 sediment samples explored across SSK42/5 and SSK42/6 were used individually as templates to PCR amplify V4-V5 overlapping regions of 16S rRNA gene fragments using *Nitrosopumilus*-specific, followed by *Archaea*-specific, primers. When these PCR-products were sequenced and annotated, reads attributable to the genus *Nitrosopumilus* were identified in all the 25 experimental sets (Table S21).

DISCUSSION

Wide spread of the new isolates and their phylogenetic relatives across the marine realm

High levels of correspondence witnessed among the metagenomes and metatranscriptomes sequenced along SSK42/5 and SSK42/6 on one hand and the genomes of the new chemoorganotrophic isolates on the other illustrated the ubiquitous presence and activity of the strains across the ASOMZ sediment horizon explored (Tables S14 and S16). At the same time, literature survey showed that close phylogenetic relatives of the OMZ-sediment isolates were widespread in diverse marine habitats. For instance, *Brevibacterium* species (Bhadra et al. 2008; Chen et al. 2016; Pie et al. 2020) have been retrieved from deep subsurfaces of the Pacific and Indian Oceans. Strains of *Brucella* have been retrieved from the deep subsurface of the Atlantic Ocean (Odumosu et al. 2020), while halotolerant strains of the genus have also been unearthed from lacustrine sediments (Nshimiyimana et al. 2020). *Gordonia* species have been retrieved from the sediments of marine tidal flats (Kim et al. 2019) and mangrove vegetations (Sangkanu et al. 2019). Whereas members of *Halomonas* (Xu et al. 2013; Wang et al. 2021), *Halopseudomonas* (Wang and Sun 2016; Bollinger et al. 2020; Rudra and Gupta 2021) and *Mesobacillus* (Yoon et al. 2001; Pal et al. 2017) are extensively present, *Marinobacter* are often predominant (Guo et al. 2007; Handley et al. 2009; Gorshkova et al. 2003; Gao et al. 2013), within the microbiota across diverse marine ecosystems, including the sedimentary ones. *Stenotrophomonas* strains also are not alien to the marine realm (Reina et

al. 2019; Salas-Ovilla et al. 2019). All these facts collectively point towards a very comprehensive role of these bacterial genera in marine carbon cycling, across different geographical and geochemical regimes. Especially, in the context of sediment biogeochemistry within continental shelf/slope territories, these bacteria - by virtue of being adept to remineralizing complex carbon compounds under aerobic to microaerobic conditions – appear to be important determinants of simple fatty acids availability for the downstream anaerobic metabolisms of the carbon-sulfur cycle.

Quorum-based extreme oligotrophy as a key adaptive trait of chemoorganoheterotrophic bacteria in shelf/slope sediments

Deposition from overlying water-columns constitutes the only means of organic carbon and oxidant input for marine subsurface ecosystems within shelf/slope territories (Sarkar et al. 2022). Although the seafloor in the upwelling regions and OMZs of the global ocean receive copious organic matter from the highly productive water-columns, down the sediment depths the microbiomes get increasingly constrained for utilizable sources of energy, electron and carbon, plus those of electron acceptors or respiratory substrates (Arndt et al. 2013; Lever et al. 2015; Fernandes et al. 2018). Not only O_2, but also the other oxidants (terminal electron acceptors), which are capable of acting as respiratory substrates in different microorganisms (for example, nitrate, manganic, and ferric ions), get depleted within relatively shallow sediment depths; simultaneously, in the diagenetically maturing deeper sediments, the remnant organic matter becomes progressively refractory towards catabolic breakdown by chemoorganoheterotrophic bacteria (Canfield 1994; Seiter et al. 2005; Burdige 2007; Komada et al. 2016). While in any rapidly changing physicochemical milieu, adaptive responses of bacterial communities determine their resilience and survival value (Lauro et al. 2009), amid acute starvation, an initial increase in cell number followed by a prolonged retention of the same is considered to be a common survival strategy (Amy and Morita 1983). In the biogeochemical context of shelf/slope sediments, sensing the population level and maintaining a fixed cell density post onset of starvation, as observed in the axenic culture for all the nine OMZ isolates, could be a key quality ensuring survival in deeper horizons. Notably, for all the present isolates, oligotrophic growth, starting with 10^3 cells ml^{-1} of the culture medium, stopped when a density of 10^4 or 10^5 cells ml^{-1} was reached after 96 hours of incubation; thereafter, the cell density remained unchanged even after prolonged incubation (Table S3). While this mode of action was comparable to the standard oligotrophic behavior encountered globally

(Nimonkar et al. 2022), the phenotype of extreme oligotrophy in the OMZ-sediment isolates was further affected by the concentration of O_2 in the environment: for instance, under the microaerobic (hypoxic) condition provided, generation time got protracted for all the new isolates, and in doing so, delayed the attainment of the steady density state of 10^4 or 10^5 cells ml^{-1}. At the molecular level, signaling pathways involving autoinducer-2 are the main drivers of adaptation to carbon starvation and various other environmental stressors (McDougald et al. 2002), and the protein LuxS is involved in the secretion of autoinducer-2, the key sensor and messenger of information pertaining to cell density and nutrient concentration in the habitat. Therefore, the presence of several Lux regulon homologs in the genomes of the new isolates as well as the metagenomes of the two cores investigated could be further corroborative of a crucial role of oligotrophy in sustaining the *in situ* populations of chemoorganoheterotrophic bacteria.

Nitrate/nitrate reduction, and fermentation, as potential means of coping hypoxia

From the physiological characterizations carried out thus far, seven out of the nine ASOMZ-sediment isolates appeared to be obligately aerobic, whereas only two strains, namely *B. anthropi* JSBI001 and *H. bauzanensis* SMJS2, were found to be facultatively anaerobic with abilities to grow on yeast extract or acetate via nitrate and/or nitrite reduction in the absence of O_2. While the genomic contents of these two strains corroborated their nitrate-/nitrite-respiring phenotypes, three more new isolates, namely *Halomonas* sp. BDJS001, *M. segnicrescens* AN1 and *Mesobacillus* sp. SBJS01, despite exhibiting no such phenotype in chemoorganoheterotrophic medium based on yeast extract or acetate, did possess the genes that are necessary for respiring nitrate/nitrite to dinitrogen, ammonia or nitrous oxide. Therefore, possibilities remain that the nitrate/nitrite reduction capabilities of these organisms are coupled with some hitherto unknown catabolic processes that utilize substrates other than those which were tested in this present study. In such a scenario too, there remain four ASOMZ-sediment isolates (*Brevibacterium* strains BDJS002 and JSBI002, *G. hongkongensis* SMJS1, and *S. maltophilia* SBJS02) whose survival in the sulfidic (anoxic) habitat (Fernandes et al. 2018) is unexplainable by the biogeochemical data available for this ecosystem.

In the above context it is noteworthy that all the new strains isolated from the ASOMZ sediments could maintain a fraction of their cell population over prolonged anaerobic incubation by means of fermentative metabolism (Fig. 1 and Table S1). Obligately aerobic bacteria, across taxonomies and ecologies, are known to withstand O_2 limitation by using

various fermentative metabolisms, sometimes in conjunction with nitrate reduction. For instance, the soil-dwelling obligate aerobe *Mycobacterium smegmatis* activates the fermentative production of hydrogen to overcome the reductive stress emanating from dwindling O_2 in the chemical milieu (Berney et al. 2014). During hypoxia-induced fermentation, the organism channelizes organic carbon through the Pentose phosphate and Entner-Doudoroff pathways, excretes copious hydrogen, and accumulates glycerides so as to be able to recommence growth when O_2 is again available (Gillett et al. 2023). The opportunistic pathogen *Pseudomonas aeruginosa* can respire nitrate, and ferment arginine, but when these substrates are not available in the chemical milieu, pyruvate fermentation to acetate via acetyl-CoA helps it survive without growth under long spells of anoxia (Eschbach et al. 2004). *Shewanella oneidensis* can survive anoxia via pyruvate fermentation when other electron acceptors are unavailable (Pinchuk et al. 2011). The obligate aerobe *Streptomyces coelicolor* can grow under microaerobic conditions and survive several weeks under anoxia; they have potentials for the fermentation of pyruvate to acetate via acetyl-CoA (Van Keulen et al. 2007). Though unable to render anaerobic growth by dissimilatory nitrate reduction, the organism employs its respiratory nitrate reductases (Nar proteins) for the maintenance of proton motive force and redox balance across the cell membrane under anoxic conditions (Fischer et al. 2010; Falke et al. 2019). The above information, in conjunction with the current data, points towards a multifaceted metabolic role of nitrate reduction and fermentation in the sustenance of aerobic bacteria within the sulfidic (anoxic) sediments of the ASOMZ. However, further studies of pure-culture, as well as culture-independent, microbiology would be required at the level of the omics (transcriptomics, proteomics, and/or metabolomics) to establish the exact scopes of these metabolic processes *in situ*. Such information can subsequently be used to determine the actual biogeochemical implications that these processes potentially hold for *in situ* carbon cycling.

NO dismutation, and other potential sources, of cryptic O_2 for aerobic bacteria in OMZ sediments

The present state of knowledge does not offer any experimental insight to the absence or presence of O_2 (at whatever miniscule concentration that may be) in the ASOMZ sediment system. Nevertheless, some explanation needs to be put forth (for subsequent testing) with regard to how the isolated aerobic chemoorganoheterotrophs having neither anaerobic respiration capabilities nor fermentative growth potentials could be active, and relatively

abundant, in these extremely reduced (sulfide-containing) sediments (Fernandes et al. 2018) which also have less probability of O_2 influx, compared with other shelf/slope sediment systems that are situated outside of OMZ territories. As for the nearly anoxic conditions of OMZ waters, feasibility of active aerobic metabolism *in situ* has been attributed to local oxygenic photosynthesis (Tiano et al. 2014; Garcia-Robledo et al. 2017), and prompt response of community metabolism to brisk spatiotemporal fluctuations in the availability of O_2 (Dalsgaard et al. 2014). Furthermore, biogenic O_2 produced via dismutation of chlorite has been hypothesized, based on metagenomic footprints and results of co-culture experiments, to sustain aerobic microorganisms in anoxic/hypoxic aquifers (Ruff et al. 2023), as well as the same ASOMZ sediment system (Bhattacharya et al. 2020) on which the present study was based. Notably, however, no oxyanion of chlorine (perchlorate, chlorate, or chlorite) was detected in either of the two ecosystems.

NO dismutation is also a potential source of biogenic O_2 in deep subsurface microbiomes (Ettwig et al. 2010; Kraft et al. 2022; Ruff et al. 2023). NO dismutases of archaea (Kraft et al. 2022) and bacteria (Ettwig et al. 2010) apparently convert NO to N_2 and O_2, with or without forming N_2O as an intermediate, respectively. Notably, in both the processes the substrate NO is derived from the reduction of nitrite (NO_2^-), which in turn, however, is an intermediate of denitrification (NO_3^- reduction) in the bacteria, and a derivative of aerobic NH_3 oxidation in the archaea. In biogeochemical context of SSK42/5 and SSK42/6, the NO dismutation mechanism encountered in aerobic NH_3-oxidizing archaea (such as *N*. *maritimus*) seems to be more feasible *in situ*, as the sediments are redox-stratified and largely unbioturbated, so NO_3^- is typically restricted to the surface and near-surface territories, whereas NH_3 prevails at increasingly high concentrations along the sediment depths due to hectic organic matter remineralization (Fernandes et al. 2018). Indeed, along SSK42/5 and SSK42/6, the presence of *Nitrosopumilus* species, including *N*. *maritimus*, was corroborated by CDSs annotated within the assembled metagenomes (Fig. 8 and Table S19). The occurrence of the genus in this sediment system was further evidenced by the analysis of PCR-amplified 16S rRNA gene sequences (Table S21). The assembled metagenomes of all the sediment samples analyzed from this ecosystem, except 220 cmbsf and 265 cmbsf of SSK42/6, also contained CDSs for nitric oxide dismutase (Table S20).

Nitrosopumilus and other ammonia-oxidizing archaea are widely distributed in the global ocean, and their habitats include seawaters and sediments having O_2 concentration below the detection limit of current technologies (Karner et al. 2001; Könneke et al. 2005; Molina et al.

2010; Beman et al. 2012; Stewart et al. 2012; Sollai et al. 2019). This, in conjunction with the discovery of an NO dismutation phenotype in *Pseudomonas aeruginosa* that releases up to 20 µM O_2 to the extracellular milieu (Lichtenberg et al. 2021), and the identification of nitric oxide dismutase genes in taxonomically diverse bacteria (Murali et al. 2022; Ruff et al. 2023), suggests that the molecular attribute of O_2 generation during ammonia oxidation could be widespread across the taxonomic as well as ecological spectra. So far as NO dismutation by *N*. *maritimus* is concerned, upon onset of anoxia in the environment, aerobic ammonia oxidation generate N_2 and O_2 via NO_2^-, NO, and then N_2O; subsequently, the O_2 produced can not only act as the electron acceptor for restarting aerobic oxidation of ammonia but also can be potentially released to the cells' external chemical milieu (Kraft et al. 2022). So, whereas it is tempting to hypothesize that within these apparently anoxic (sulfidic) sedimentary environments, potential close association with cells of *Nitrosopumilus* could be a viable means of O_2 for other obligate aerobes present *in situ*, only future experiments involving anaerobic co-cultures can ascertain whether *Nitrosopumilus* strains can indeed produce and transmit such surplus O_2 that can sustain other aerobic microorganisms as well.

Potential role of the aerobic chemoorganoheterotrophs in the carbon cycle of ASOMZ sediments

The sediment horizon explored in the present study of pure culture, as well as omics-based, microbiology is situated off the west coast of Indian, and is impinged by the acutely hypoxic waters of the Arabian Sea OMZ. In this kind of marine biogeochemical systems, water column productivity and organic carbon deposition to the seafloor are both very high; abundant complex organic matter is delivered to the seabed (Cavan et al. 2017; Jessen et al. 2017) since low concentrations of dissolved O_2 in the overlying waters limit their biodegradation prior to deposition (Revsbech et al. 2009; Ulloa et al. 2012; Garcia-Robledo et al. 2017). Subsequently, within the sedimentary realm, notwithstanding the apparent dearth of respiratory oxidants (terminal electron acceptors) having high reduction potential, efficient remineralization is noted for almost the entire organic carbon deposited (Cavan et al. 2017; Fernandes et al. 2018). Furthermore, it is remarkable that the catabolic degradation of complex carbon compounds in these sediment regimes takes place hand in hand with anaerobic microbial metabolisms that are dependent on the utilization of simple fatty acids as carbon source (van der Weijden et al. 1999; Schulte et al. 2000; Seiter et al. 2005; Bowles et al. 2014; Cowie et al. 2014; Fernandes et al. 2018; Ruvalcaba et al. 2020). Hectic activities of anaerobic life

processes in the surface and near-surface sediments is attributed to low sedimentation rates affording high O_2-exposure time for the degradation of organic carbon in the surficial sediments despite acute hypoxia in the benthic waters (Bhattacharya et al. 2021). So far as the sites SSK42/5 and SSK42/6, underlying the approximate midpoint of the vertical span of the ASOMZ, are concerned, copious organic matter deposition takes place at the sediment surface (organic matter constituted around 4% of the total sediment weight in the first few 10s cmbsf), while steady depletion of the total organic carbon content to ≤1% of the total sediment weight happens within a few 100s cmbsf (Fernandes et al. 2018). This gradual depletion trend is reflective of the fact that considerable proportions of the total organic carbon deposited to the seabed from the water column is degraded through the diagenetically matured, older and deeper, sediment layers amid an accentuating scarcity of oxidants down the sediment depth. It is specifically in this biogeochemical context that the chemoorganoheterotrophic bacteria revealed in this study (alongside their physiological comparators that are also present *in situ*) emerge as the key players of carbon cycling in the ASOMZ sediments. Their versatile abilities to (i) catabolize, and grow on, complex organic compounds of both marine and terrestrial origin via aerobic respiration at low (as well as high) O_2 concentration, (ii) grow anaerobically by reducing nitrate and/or nitrite, (iii) preserve a fraction of the cell population via fermentative metabolism under anaerobic condition, and (iv) grow by means of extreme oligotrophy at a low cell density amid low (and high) O_2 concentration, make them fit for prolonged carbon remineralization across the sediment horizon by utilizing whatever small amount of oxidants is available in time and space.

SUPPLEMENTARY DATA

Supplementary information and data are available online.

DATA AVAILABILITY

All nucleotide sequence data have been deposited in NCBI Sequence Read Archive (SRA) or GenBank under the BioProject accession number PRJNA309469:

The complete circular genome or plasmid sequences of the pure culture strains isolated have the GenBank accession numbers CP109811, CP109812, CP110339 through CP110342, CP110535, CP116392, CP123381 through CP123383, CP123445, and CP123446.

The whole metagenome shotgun sequence datasets have the Run Accession numbers SRR3646127, SRR3646128, SRR3646129, SRR3646130, SRR3646131, SRR3646132,

SRR3646144, SRR3646145, SRR3646147, SRR3646148, SRR3646150, SRR3646151, SRR3646152, SRR3646153, SRR3646155, SRR3646156, SRR3646157, SRR3646158, SRR3646160, SRR3646161, SRR3646162, SRR3646163, SRR3646164, SRR3646165; SRR3570036, SRR3570038, SRR3577067, SRR3577068, SRR3577070, SRR3577071, SRR3577073, SRR3577076, SRR3577078, SRR3577079, SRR3577081, SRR3577082, SRR3577086, SRR3577087, SRR3577090, SRR3577311, SRR3577337, SRR3577338, SRR3577341, SRR3577343, SRR3577344, SRR3577345, SRR3577347, SRR3577349, SRR3577350, and SRR3577351.

The whole metatranscriptome shotgun sequence datasets have the Run Accession numbers SRR7967962, SRR9596399, SRR7983762, SRR9597791, and SRR7992674.

The sequence datasets obtained via PCR amplification of the V4-V5 regions of *Nitrosopumilus*-specific 16S rRNA genes have the Run Accession numbers SRR24121604, SRR24121705, SRR24121602, SRR24121623, SRR24123082, SRR24122693, SRR24121664, SRR24121706, SRR24121641, SRR24121637, SRR24121644, SRR24121647, SRR24121642, SRR24122688, SRR24122690, SRR24121638, SRR24121640, SRR24121648, SRR24121663, SRR24121649, SRR24121645, SRR24123085, SRR24122686, SRR24121636, and SRR24121643.

ACKNOWLEDGEMENTS

We express gratitude to the Director of CSIR-National Institute of Oceanography for enabling the research cruise SSK42. Support extended by the CSIR-NIO Ship Cell and crew members of SSK42 is recognized gratefully. J.S. and S.D. received fellowships from Council of Scientific and Industrial Research, Government of India (GoI). M.M. and S.C. received fellowships from the Department of Biotechnology, GoI. S.B., N.M. and S.N. got their fellowships from Bose Institute.

AUTHOR CONTRIBUTIONS

W.G. conceived the study, designed the experiments, interpreted the results, and wrote the paper. J.S. planned and performed the experiments, analyzed and curated the data, and also composed the paper. A.M. led the SSK42 mission and all geochemical studies therein; A.M. and A.P. made intellectual contributions to the present paper. M.M. performed microbiological experiments, while S.B., S.C., N.M., S.D. and S.N. performed omics studies. All authors read and ratified the manuscript.

FUNDING

The microbiological studies were funded by Bose Institute (via Intramural Faculty Grants) and Earth System Science Organization, Ministry of Earth Sciences (MoES), GoI via the extramural grant MoES/36/00IS/Extra/19/2013; the research cruise SSK42 was also funded by MoES (GAP2303).

COMPETING INTEREST

The authors declare no competing interest.

REFERENCES

Acharya SS, Panigrahi MK (2016) Eastward shift and maintenance of Arabian Sea oxygen minimum zone: Understanding the paradox. Deep Sea Res Part I: Oceanogr Res Pap 115:240-252. https://doi.org/10.1016/j.dsr.2016.07.004

Aller RC, Blair NE (2004) Early diagenetic remineralization of sedimentary organic C in the Gulf of Papua deltaic complex (Papua New Guinea): Net loss of terrestrial C and diagenetic fractionation of C isotopes. Geochim Cosmochim Acta 68:1815-1825. https://doi.org/10.1016/j.gca.2003.10.028

Amy PS, Morita RY (1983) Starvation-survival patterns of sixteen freshly isolated open-ocean bacteria. Appl Environ Microbiol 45:1109-1115. https://doi.org/10.1128/aem.45.3.1109-1115.1983

Anand AA et al. (2010) Isolation and characterization of bacteria from the gut of *Bombyx mori* that degrade cellulose, xylan, pectin and starch and their impact on digestion. J Insect Sci 10:107. https://doi.org/10.1673/031.010.10701

Arndt S, Jørgensen BB, LaRowe DE, Middelburg JJ, Pancost RD, Regnier P (2013) Quantifying the degradation of organic matter in marine sediments: A review and synthesis. Earth Sci Rev 123:53-86. https://doi.org/10.1016/j.earscirev.2013.02.008

Baker GC, Smith JJ, Cowan DA (2003) Review and re-analysis of domain-specific 16S primers. J Microbiol Methods 55:541-555. https://doi.org/10.1016/j.mimet.2003.08.009

Bange HW, Naqvi SWA, Codispoti LA (2005) The nitrogen cycle in the Arabian Sea. Prog Oceanogr 65:145-158. https://doi.org/10.1016/j.pocean.2005.03.002

Banse K, Naqvi SWA, Narvekar PV, Postel JR, Jayakumar DA (2014) Oxygen minimum zone of the open Arabian Sea: variability of oxygen and nitrite from daily to decadal timescales. Biogeosciences 11:2237-2261. https://doi.org/10.5194/bg-11-2237-2014

Beman JM, Bertics VJ, Braunschweiler T, Wilson JM (2012) Quantification of ammonia oxidation rates and the distribution of ammonia-oxidizing Archaea and Bacteria in marine sediment depth profiles from Catalina Island, California. Front Microbiol 3:263. https://doi.org/10.3389/fmicb.2012.00263

Berney M, Greening C, Conrad R, Jacobs WR, Jr., Cook GM (2014) An obligately aerobic soil bacterium activates fermentative hydrogen production to survive reductive stress during hypoxia. Proc Natl Acad Sci USA 111:11479-11484. https://doi.org/10.1073/pnas.1407034111

Bhadra B, Raghukumar C, Pindi PK, Shivaji S (2008) *Brevibacterium oceani* sp. nov., isolated from deep-sea sediment of the Chagos Trench, Indian Ocean. Int J Syst Evol Microbiol 58:57-60. https://doi.org/10.1099/ijs.0.64869-0

Bhattacharya S, Mapder T, Fernandes S, Roy C, Sarkar J, Rameez MJ et al (2021) Sedimentation rate and organic matter dynamics shape microbiomes across a continental margin. Biogeosciences 18:5203-5222. https://doi.org/10.5194/bg-18-5203-2021

Bhattacharya S, Roy C, Mandal S, Sarkar J, Rameez MJ, Mondal N et al (2020) Aerobic microbial communities in the sediments of a marine oxygen minimum zone. FEMS Microbiol Lett 367. https://doi.org/10.1093/femsle/fnaa157

Bollinger A, Thies S, Katzke N, Jaeger KE (2020) The biotechnological potential of marine bacteria in the novel lineage of *Pseudomonas pertucinogena*. Microb Biotechnol 13:19-31. https://doi.org/10.1111/1751-7915.13288

Bowles MW, Mogollón JM, Kasten S, Zabel M, Hinrichs KU (2014) Global rates of marine sulfate reduction and implications for sub-sea-floor metabolic activities. Science 344:889-891. https://doi.org/10.1126/science.1249213

Burdige DJ (2007) Preservation of Organic Matter in Marine Sediments: Controls, Mechanisms, and an Imbalance in Sediment Organic Carbon Budgets? Chem Rev 107:467-485. https://doi.org/10.1021/cr050347q

Canfield DE (1994) Factors influencing organic carbon preservation in marine sediments.

Chem Geol 114:315-329. https://doi.org/10.1016/0009-2541(94)90061-2

Cantalapiedra CP, Hernández-Plaza A, Letunic I, Bork P, Huerta-Cepas J (2021) eggNOG-mapper v2: Functional Annotation, Orthology Assignments, and Domain Prediction at the Metagenomic Scale. Mol Biol Evol 38:5825-5829. https://doi.org/10.1093/molbev/msab293

Cavan EL, Trimmer M, Shelley F, Sanders R (2017) Remineralization of particulate organic carbon in an ocean oxygen minimum zone. Nat Commun 8:14847. https://doi.org/10.1038/ncomms14847

Chen P, Zhang L, Wang J, Ruan J, Han X, Huang Y (2016) *Brevibacterium sediminis* sp. *nov*., isolated from deep-sea sediments from the Carlsberg and Southwest Indian Ridges. Int J Syst Evol Microbiol 66:5268-5274. https://doi.org/10.1099/ijsem.0.001506

Cocaign-Bousquet M, Garrigues C, Loubiere P, Lindley ND (1996) Physiology of pyruvate metabolism in Lactococcus lactis. Antonie Van Leeuwenhoek 70:253-267. https://doi.org/10.1007/bf00395936

Cowie G, Mowbray S, Kurian S, Sarkar A, White C, Anderson A et al (2014) Comparative organic geochemistry of Indian margin (Arabian Sea) sediments: estuary to continental slope. Biogeosciences 11:6683-6696. https://doi.org/10.5194/bg-11-6683-2014

Cowie GL, Hedges JI, Calvert SE (1992) Sources and relative reactivities of amino acids, neutral sugars, and lignin in an intermittently anoxic marine environment. Geochim Cosmochim Acta 56:1963-1978. https://doi.org/10.1016/0016-7037(92)90323-B

Crocetti GR, Hugenholtz P, Bond PL, Schuler A, Keller J, Jenkins D et al (2000) Identification of Polyphosphate-Accumulating Organisms and Design of 16S rRNA-Directed Probes for Their Detection and Quantitation. Appl Environ Microbiol 66:1175-1182. https://doi.org/10.1128/AEM.66.3.1175-1182.2000

Dalsgaard T, Stewart FJ, Thamdrup B, De Brabandere L, Revsbech NP, Ulloa O et al (2014) Oxygen at nanomolar levels reversibly suppresses process rates and gene expression in anammox and denitrification in the oxygen minimum zone off northern Chile. MBio 5(6):10-128. https://doi.org/10.1128/mbio.01966-14

Eschbach M, Schreiber K, Trunk K, Buer J, Jahn D, Schobert M (2004) Long-term anaerobic survival of the opportunistic pathogen *Pseudomonas aeruginosa* via pyruvate fermentation. J

Bacteriol 186:4596-4604. https://doi.org/10.1128/jb.186.14.4596-4604.2004

Ettwig KF, Butler MK, Le Paslier D, Pelletier E, Mangenot S, Kuypers MM et al (2010) Nitrite-driven anaerobic methane oxidation by oxygenic bacteria. Nature 464(7288):543-548. https://doi.org/10.1038/nature08883

Falke D, Biefel B, Haase A, Franke S, Fischer M, Sawers RG (2019) Activity of Spore-Specific Respiratory Nitrate Reductase 1 of *Streptomyces coelicolor* A3(2) Requires a Functional Cytochrome bcc-aa(3) Oxidase Supercomplex. J Bacteriol 201. https://doi.org/10.1128/jb.00104-19

Fernandes S, Mazumdar A, Bhattacharya S, Peketi A, Mapder T, Roy R et al (2018) Enhanced carbon-sulfur cycling in the sediments of Arabian Sea oxygen minimum zone center. Sci Rep 8:8665. https://doi.org/10.1038/s41598-018-27002-2

Fischer M, Alderson J, van Keulen G, White J, Sawers RG (2010) The obligate aerobe *Streptomyces coelicolor* A3(2) synthesizes three active respiratory nitrate reductases. Microbiology (Reading) 156:3166-3179. https://doi.org/10.1099/mic.0.042572-0

Gao W, Cui Z, Li Q, Xu G, Jia X, Zheng L (2013) *Marinobacter nanhaiticus* sp. *nov*., polycyclic aromatic hydrocarbon-degrading bacterium isolated from the sediment of the South China Sea. Antonie Van Leeuwenhoek 103:485-491. https://doi.org/10.1007/s10482-012-9830-z

Garcia-Robledo E, Padilla CC, Aldunate M, Stewart FJ, Ulloa O, Paulmier A et al (2017) Cryptic oxygen cycling in anoxic marine zones. Proc Natl Acad Sci USA 114:8319-8324. https://doi.org/10.1073/pnas.1619844114

Ghosh W, Mandal S, Roy P (2006) *Paracoccus bengalensis* sp. *nov*., a novel sulfur-oxidizing chemolithoautotroph from the rhizospheric soil of an Indian tropical leguminous plant. Syst Appl Microbiol 29:396-403. https://doi.org/10.1016/j.syapm.2005.10.004

Gillett DL, Hutchinson T, Mudaliyar M, Watts TD, Wong WW, Locop J et al (2023) An obligate aerobe adapts to hypoxia by hybridising fermentation with carbon storage.2023.2009.2011.557286. https://doi.org/10.1101/2023.09.11.557286 %J bioRxiv

Gobet A, Barbeyron T, Matard-Mann M, Magdelenat G, Vallenet D, Duchaud E et al (2018) Evolutionary Evidence of Algal Polysaccharide Degradation Acquisition by *Pseudoalteromonas carrageenovora* 9(T) to Adapt to Macroalgal Niches. Front Microbiol 9:2740.

https://doi.org/10.3389/fmicb.2018.02740

Gorshkova NM, Ivanova EP, Sergeev AF, Zhukova NV, Alexeeva Y, Wright JP et al (2003) *Marinobacter excellens* sp. nov., isolated from sediments of the Sea of Japan. Int J Syst Evol Microbiol 53:2073-2078. https://doi.org/10.1099/ijs.0.02693-0

Guo B, Gu J, Ye YG, Tang YQ, Kida K, Wu XL (2007) *Marinobacter segnicrescens* sp. nov., a moderate halophile isolated from benthic sediment of the South China Sea. Int J Syst Evol Microbiol 57:1970-1974. https://doi.org/10.1099/ijs.0.65030-0

Handley KM, Héry M, Lloyd JR (2009) *Marinobacter santoriniensis* sp. nov., an arsenate-respiring and arsenite-oxidizing bacterium isolated from hydrothermal sediment. Int J Syst Evol Microbiol 59:886-892. https://doi.org/10.1099/ijs.0.003145-0

Helly JJ, Levin LA (2004) Global distribution of naturally occurring marine hypoxia on continental margins. Deep Sea Res Part I: Oceanogr Res Pap 51:1159-1168. https://doi.org/10.1016/j.dsr.2004.03.009

Hoshino T, Doi H, Uramoto GI, Wörmer L, Adhikari RR, Xiao N et al (2020) Global diversity of microbial communities in marine sediment. Proc Natl Acad Sci USA 117:27587-27597. https://doi.org/10.1073/pnas.1919139117

Hosoda A, Sakai M, Kanazawa S (2003) Isolation and characterization of agar-degrading *Paenibacillus* spp. associated with the rhizosphere of spinach. Biosci Biotechnol Biochem 67:1048-1055. https://doi.org/10.1271/bbb.67.1048

Huerta-Cepas J, Szklarczyk D, Heller D, Hernández-Plaza A, Forslund SK, Cook H et al (2019) eggNOG 5.0: a hierarchical, functionally and phylogenetically annotated orthology resource based on 5090 organisms and 2502 viruses. Nucleic Acids Res 47:D309-d314. https://doi.org/10.1093/nar/gky1085

Hyatt D, Chen GL, Locascio PF, Land ML, Larimer FW, Hauser LJ (2010) Prodigal: prokaryotic gene recognition and translation initiation site identification. BMC Bioinform 11:119. https://doi.org/10.1186/1471-2105-11-119

Jayakumar DA, Chris AF, Naqvi SWA, Bess BW (2004) Diversity of nitrite reductase genes (nirS) in the denitrifying water column of the coastal Arabian Sea. Aquat Microb Ecol 34:69-78

Jegatheesan A, Sudhakar MP, Poonam C, Perumal K, Arunkumar K (2017) Isolation and characterization of alginate-degrading bacteria *Sinomicrobium oceani*. Biomass Convers Biorefin 7:51-58. https://doi.org/10.1007/s13399-016-0212-z

Jessen GL, Lichtschlag A, Ramette A, Pantoja S, Rossel PE, Schubert CJ et al (2017) Hypoxia causes preservation of labile organic matter and changes seafloor microbial community composition (Black Sea). Sci Adv 3:e1601897. https://doi.org/10.1126/sciadv.1601897

Jørgensen BB, Wenzhöfer F, Egger M, Glud RN (2022) Sediment oxygen consumption: Role in the global marine carbon cycle. Earth Sci Rev 228:103987. https://doi.org/10.1016/j.earscirev.2022.103987

Kallmeyer J, Pockalny R, Adhikari RR, Smith DC, D'Hondt S (2012) Global distribution of microbial abundance and biomass in subseafloor sediment. Proc Natl Acad Sci USA 109:16213-16216. https://doi.org/10.1073/pnas.1203849109

Kalvelage T, Lavik G, Jensen MM, Revsbech NP, Löscher C, Schunck H et al (2015) Aerobic microbial respiration in oceanic oxygen minimum zones. PloS one 10(7):e0133526. https://doi.org/10.1371/journal.pone.0133526

Karner MB, DeLong EF, Karl DM (2001) Archaeal dominance in the mesopelagic zone of the Pacific Ocean. Nature 409:507-510. https://doi.org/10.1038/35054051

Kim HS, Dong K, Kim J, Lee SS (2019) Characteristics of crude oil-degrading bacteria *Gordonia iterans* isolated from marine coastal in Taean sediment. Microbiologyopen 8:e00754. https://doi.org/10.1002/mbo3.754

Komada T, Burdige DJ, Li H-L, Magen C, Chanton JP, Cada AK (2016) Organic matter cycling across the sulfate-methane transition zone of the Santa Barbara Basin, California Borderland. Geochim Cosmochim Acta 176:259-278. https://doi.org/10.1016/j.gca.2015.12.022

Könneke M, Bernhard AE, de la Torre JR, Walker CB, Waterbury JB, Stahl DA (2005) Isolation of an autotrophic ammonia-oxidizing marine archaeon. Nature 437:543-546. https://doi.org/10.1038/nature03911

Kraft B, Jehmlich N, Larsen M, Bristow LA, Könneke M, Thamdrup B et al (2022) Oxygen and nitrogen production by an ammonia-oxidizing archaeon. Science 375:97-100. https://doi.org/10.1126/science.abe6733

Kristensen E, Ahmed SI, Devol AH (1995) Aerobic and anaerobic decomposition of organic matter in marine sediment: Which is fastest? Limnol Oceanogr 40:1430-1437. https://doi.org/10.4319/lo.1995.40.8.1430

Lam P, Kuypers MM (2011) Microbial nitrogen cycling processes in oxygen minimum zones. Ann Rev Mar Sci 3:317-345. https://doi.org/10.1146/annurev-marine-120709-142814

Langmead B, Salzberg SL (2012) Fast gapped-read alignment with Bowtie 2. Nat Methods 9:357-359. https://doi.org/10.1038/nmeth.1923

Lauro FM, McDougald D, Thomas T, Williams TJ, Egan S, Rice S et al (2009) The genomic basis of trophic strategy in marine bacteria. Proc Natl Acad Sci USA 106:15527-15533. https://doi.org/10.1073/pnas.0903507106

Lever MA, Rogers KL, Lloyd KG, Overmann J, Schink B, Thauer RK et al (2015) Life under extreme energy limitation: a synthesis of laboratory- and field-based investigations. FEMS Microbiol Rev 39:688-728. https://doi.org/10.1093/femsre/fuv020

Li D, Liu CM, Luo R, Sadakane K, Lam TW (2015) MEGAHIT: an ultra-fast single-node solution for large and complex metagenomics assembly via succinct de Bruijn graph. Bioinformatics 31:1674-1676. https://doi.org/10.1093/bioinformatics/btv033

Lichtenberg M, Line L, Schrameyer V, Jakobsen TH, Rybtke ML, Toyofuku M et al (2021) Nitric-oxide-driven oxygen release in anoxic Pseudomonas aeruginosa. Iscience. 17:24. https://doi.org/10.1016/j.isci.2021.103404

Long AM, Jurgensen SK, Petchel AR, Savoie ER, Brum JR (2021) Microbial Ecology of Oxygen Minimum Zones Amidst Ocean Deoxygenation. Front Microbiol 12:748961. https://doi.org/10.3389/fmicb.2021.748961

Mandal S, Bhattacharya S, Roy C, Rameez MJ, Sarkar J, Mapder T et al (2020) Cryptic roles of tetrathionate in the sulfur cycle of marine sediments: microbial drivers and indicators. Biogeosciences 17:4611-4631. https://doi.org/10.5194/bg-17-4611-2020

McDougald D, Gong L, Srinivasan S, Hild E, Thompson L, Takayama K et al (2002) Defences against oxidative stress during starvation in bacteria. Antonie Van Leeuwenhoek 81:3-13. https://doi.org/10.1023/a:1020540503200

Meier-Kolthoff JP, Göker M (2019) TYGS is an automated high-throughput platform for state-of-the-art genome-based taxonomy. Nat Commun 10:2182. https://doi.org/10.1038/s41467-019-10210-3

Middelburg JJ (2019) Carbon Processing at the Seafloor. In: Middelburg JJ (ed) Marine Carbon Biogeochemistry: A Primer for Earth System Scientists. Springer International Publishing, Cham, pp 57-75

Molina V, Belmar L, Ulloa O (2010) High diversity of ammonia-oxidizing archaea in permanent and seasonal oxygen-deficient waters of the eastern South Pacific. Environ Microbiol 12:2450-2465. https://doi.org/10.1111/j.1462-2920.2010.02218.x

Mondal N, Peketi A, Mapder T, Roy C, Mazumdar A, Chakraborty R et al (2022) Indus and Nubra Valley hot springs affirm the geomicrobiological specialties of Trans-Himalayan hydrothermal systems. J Earth Syst Sci 131:12. https://doi.org/10.1007/s12040-021-01757-1

Moreno R, Rojo F (2008) The target for the Pseudomonas putida Crc global regulator in the benzoate degradation pathway is the BenR transcriptional regulator. J Bacteriol 190:1539-1545. https://doi.org/10.1128/jb.01604-07

Moriya Y, Itoh M, Okuda S, Yoshizawa AC, Kanehisa M (2007) KAAS: an automatic genome annotation and pathway reconstruction server. Nucleic Acids Res 35:W182-185. https://doi.org/10.1093/nar/gkm321

Murali R, Hemp J, Gennis RB (2022) Evolution of quinol oxidation within the heme copper oxidoreductase superfamily. Biochim Biophys Acta Bioenerg 1863(8):148907. https://doi.org/10.1016/j.bbabio.2022.148907

Naqvi SW, Naik H, Pratihary A, D'souza W, Narvekar PV, Jayakumar DA et al (2006) Coastal versus open-ocean denitrification in the Arabian Sea. Biogeosciences 3:621-633. https://doi.org/10.5194/bg-3-621-2006

Nimonkar YS, Godambe T, Kulkarni A, Patel T, Paul D, Paul D et al (2022) Oligotrophy vs. copiotrophy in an alkaline and saline habitat of Lonar Lake. Front Microbiol 13:939984. https://doi.org/10.3389/fmicb.2022.939984

Nshimiyimana JB, Khadka S, Zou P, Adhikari S, Proshad R, Thapa A et al (2020) Study on biodegradation kinetics of di-2-ethylhexyl phthalate by newly isolated halotolerant

Ochrobactrum anthropi strain L1-W. BMC Res Notes 13:252. https://doi.org/10.1186/s13104-020-05096-0

Odumosu BT, Augusta UN, Cano-Prieto C, Buchmann A, Nieselt K, Gross H (2020) Draft Genome Sequence of *Ochrobactrum* sp. Strain MC-1LL, a Bacterial Strain with Antimicrobial Properties, Isolated from Marine Sediments in Nigeria. Microbiol Resour Announc 9. https://doi.org/10.1128/mra.00425-20

Olaniyi OO, Yang K, Zhu YG, Cui L (2019) Heavy water-labeled Raman spectroscopy reveals carboxymethylcellulose-degrading bacteria and degradation activity at the single-cell level. Appl Microbiol Biotechnol 103:1455-1464. https://doi.org/10.1007/s00253-018-9459-6

Pal D, Mathan Kumar R, Kaur N, Kumar N, Kaur G, Singh NK et al (2017) *Bacillus maritimus* sp. nov., a novel member of the genus *Bacillus* isolated from marine sediment. Int J Syst Evol Microbiol 67:60-66. https://doi.org/10.1099/ijsem.0.001569

Pei S, Xie F, Niu S, Ma L, Zhang R, Zhang G (2020) *Brevibacterium profundi* sp. *nov*., isolated from deep-sea sediment of the Western Pacific Ocean. Int J Syst Evol Microbiol 70:5818-5823. https://doi.org/10.1099/ijsem.0.004483

Pinchuk GE, Geydebrekht OV, Hill EA, Reed JL, Konopka AE, Beliaev AS et al (2011) Pyruvate and lactate metabolism by *Shewanella oneidensis* MR-1 under fermentation, oxygen limitation, and fumarate respiration conditions. Appl Environ Microbiol 77:8234-8240. https://doi.org/10.1128/aem.05382-11

Prahl FG, De Lange GJ, Scholten S, Cowie GL (1997) A case of post-depositional aerobic degradation of terrestrial organic matter in turbidite deposits from the Madeira Abyssal Plain. Organic Geochemistry 27:141-152. https://doi.org/10.1016/S0146-6380(97)00078-8

Reina JC, Torres M, Llamas I (2019) *Stenotrophomonas maltophilia* AHL-Degrading Strains Isolated from Marine Invertebrate Microbiota Attenuate the Virulence of *Pectobacterium carotovorum* and Vibrio coralliilyticus. Mar Biotechnol (NY) 21:276-290. https://doi.org/10.1007/s10126-019-09879-w

Revsbech NP, Larsen LH, Gundersen J, Dalsgaard T, Ulloa O, Thamdrup B (2009) Determination of ultra-low oxygen concentrations in oxygen minimum zones by the STOX sensor. Limnol Oceanogr: Methods 7:371-381. https://doi.org/10.4319/lom.2009.7.371

Ruben M, Hefter J, Schubotz F, Geibert W, Butzin M, Gentz T et al (2023) Fossil organic carbon utilization in marine Arctic fjord sediments by subsurface micro-organisms. Nat Geosci 16:625-630. https://doi.org/10.1038/s41561-023-01198-z

Rudra B, Gupta RS (2021) Phylogenomic and comparative genomic analyses of species of the family Pseudomonadaceae: Proposals for the genera *Halopseudomonas* gen. *nov*. and *Atopomonas* gen. *nov*., merger of the genus *Oblitimonas* with the genus *Thiopseudomonas*, and transfer of some misclassified species of the genus *Pseudomonas* into other genera. Int J Syst Evol Microbiol 71. https://doi.org/10.1099/ijsem.0.005011

Ruff SE, Humez P, de Angelis IH, Diao M, Nightingale M, Cho S et al (2023) Hydrogen and dark oxygen drive microbial productivity in diverse groundwater ecosystems. Nat Commun 14(1):3194. https://doi.org/10.1038/s41467-023-38523-4

Ruvalcaba Baroni I, Palastanga V, Slomp CP (2020) Enhanced Organic Carbon Burial in Sediments of Oxygen Minimum Zones Upon Ocean Deoxygenation. Front Mar Sci 6. https://doi.org/10.3389/fmars.2019.00839

Saha T, Ranjan VK, Ganguli S, Thakur S, Chakraborty B, Barman P et al (2019) *Pradoshia eiseniae* gen. *nov*., sp. *nov*., a spore-forming member of the family *Bacillaceae* capable of assimilating 3-nitropropionic acid, isolated from the anterior gut of the earthworm *Eisenia fetida*. Int J Syst Evol Microbiol 69:1265-1273. https://doi.org/10.1099/ijsem.0.003304

Salas-Ovilla R, Gálvez-López D, Vázquez-Ovando A, Salvador-Figueroa M, Rosas-Quijano R (2019) Isolation and identification of marine strains of *Stenotrophomona maltophilia* with high chitinolytic activity. PeerJ 7:e6102. https://doi.org/10.7717/peerj.6102

Sangkanu S, Suriyachadkun C, Phongpaichit S (2019) Gordonia sediminis sp. nov., an actinomycete isolated from mangrove sediment. Int J Syst Evol Microbiol 69:1814-1820. https://doi.org/10.1099/ijsem.0.003399

Sarkar J, Mondal N, Mandal S, Chatterjee S, Ghosh W (2022) Deep Subsurface Microbiomes of the Marine Realm. In: Systems Biogeochemistry of Major Marine Biomes, pp 109-131

Schulte S, Mangelsdorf K, Rullkötter J (2000) Organic matter preservation on the Pakistan continental margin as revealed by biomarker geochemistry. Org Geochem 31:1005-1022. https://doi.org/10.1016/S0146-6380(00)00108-X

Seiter K, Hensen C, Zabel M (2005) Benthic carbon mineralization on a global scale. Glob Biogeochem 19. https://doi.org/10.1029/2004GB002225

Sollai M, Villanueva L, Hopmans EC, Reichart GJ, Sinninghe Damsté JS (2019) A combined lipidomic and 16S rRNA gene amplicon sequencing approach reveals archaeal sources of intact polar lipids in the stratified Black Sea water column. Geobiology 17:91-109. https://doi.org/10.1111/gbi.12316

Stewart FJ, Ulloa O, DeLong EF (2012) Microbial metatranscriptomics in a permanent marine oxygen minimum zone. Environ Microbiol 14:23-40. https://doi.org/10.1111/j.1462-2920.2010.02400.x

Stolper DA, Revsbech NP, Canfield DE (2010). Aerobic growth at nanomolar oxygen concentrations. Proc Natl Acad Sci USA 107(44):18755-18760. https://doi.org/10.1073/pnas.1013435107

Suzuki S, Kakuta M, Ishida T, Akiyama Y (2015) Faster sequence homology searches by clustering subsequences. Bioinformatics 31:1183-1190. https://doi.org/10.1093/bioinformatics/btu780

Tiano L, Garcia-Robledo E, Dalsgaard T, Devol AH, Ward BB, Ulloa O et al (2014) Oxygen distribution and aerobic respiration in the north and south eastern tropical Pacific oxygen minimum zones. Deep Sea Res. Part I Oceanogr Res Pap 94:173-183. https://doi.org/10.1016/j.dsr.2014.10.001

Ulloa O, Canfield DE, DeLong EF, Letelier RM, Stewart FJ (2012) Microbial oceanography of anoxic oxygen minimum zones. Proc Natl Acad Sci USA 109:15996-16003. https://doi.org/10.1073/pnas.1205009109

van der Weijden CH, Reichart GJ, Visser HJ (1999) Enhanced preservation of organic matter in sediments deposited within the oxygen minimum zone in the northeastern Arabian Sea. Deep Sea Research Part I: Oceanogr Res Pap 46:807-830. https://doi.org/10.1016/S0967-0637(98)00093-4

Van Keulen G, Alderson J, White J, Sawers RG (2007) The obligate aerobic actinomycete *Streptomyces coelicolor* A3(2) survives extended periods of anaerobic stress. Environ Microbiol 9:3143-3149. https://doi.org/10.1111/j.1462-2920.2007.01433.x

Van Mooy BAS, Keil RG, Devol AH (2002) Impact of suboxia on sinking particulate organic carbon: Enhanced carbon flux and preferential degradation of amino acids via denitrification. Geochim Cosmochim Acta 66:457-465. https://doi.org/10.1016/S0016-7037(01)00787-6

Wagner N, Tran QH, Richter H, Selzer PM, Unden G (2005) Pyruvate fermentation by *Oenococcus oeni* and *Leuconostoc mesenteroides* and role of pyruvate dehydrogenase in anaerobic fermentation. Appl Environ Microbiol 71:4966-4971. https://doi.org/10.1128/aem.71.9.4966-4971.2005

Wang L, Liu X, Lai Q, Gu L, Shao Z (2021) *Halomonas diversa* sp. *nov*., isolated from deep-sea sediment of the Pacific Ocean. Int J Syst Evol Microbiol 71. https://doi.org/10.1099/ijsem.0.004790

Wang MQ, Sun L (2016) *Pseudomonas oceani* sp. *nov*., isolated from deep seawater. Int J Syst Evol Microbiol 66:4250-4255. https://doi.org/10.1099/ijsem.0.001343

Wang Q, Garrity GM, Tiedje JM, Cole JR (2007) Naive Bayesian classifier for rapid assignment of rRNA sequences into the new bacterial taxonomy. Appl Environ Microbiol 73:5261-5267. https://doi.org/10.1128/aem.00062-07

Wick RR, Judd LM, Gorrie CL, Holt KE (2017) Unicycler: Resolving bacterial genome assemblies from short and long sequencing reads. PLoS Comput Biol 13:e1005595. https://doi.org/10.1371/journal.pcbi.1005595

Wright JJ, Konwar KM, Hallam SJ (2012) Microbial ecology of expanding oxygen minimum zones. Nat Rev Microbiol 10(6):381-394. https://doi.org/10.1038/nrmicro2778

Xu L, Xu XW, Meng FX, Huo YY, Oren A, Yang JY et al (2013) *Halomonas zincidurans* sp. *nov*., a heavy-metal-tolerant bacterium isolated from the deep-sea environment. Int J Syst Evol Microbiol 63:4230-4236. https://doi.org/10.1099/ijs.0.051656-0

Ye J, Coulouris G, Zaretskaya I, Cutcutache I, Rozen S, Madden TL (2012) Primer-BLAST: a tool to design target-specific primers for polymerase chain reaction. BMC Bioinform 13:134. https://doi.org/10.1186/1471-2105-13-134

Yoon JH, Kang SS, Lee KC, Kho YH, Choi SH, Kang KH et al (2001) *Bacillus jeotgali* sp. *nov*., isolated from jeotgal, Korean traditional fermented seafood. Int J Syst Evol Microbiol 51:1087-1092. https://doi.org/10.1099/00207713-51-3-1087

Zakem EJ, Mahadevan A, Lauderdale JM, Follows MJ (2020) Stable aerobic and anaerobic coexistence in anoxic marine zones. ISME J 14(1):288-301. https://doi.org/10.1038/s41396-019-0523-8

FIGURE LEGENDS

Figure 1. Growth or survival of the nine OMZ-sediment isolates in different ASW-based media under aerobic, microaerobic, or anaerobic condition. (**A**) Results of incubation in ASW_HY medium (this contained 0.5 g L^{-1} yeast extract as the energy and carbon source) for one (1D) or two (2D) days under aerobic condition. (**B**) Results of incubation in ASW_HY medium for eight days (8D) days under microaerobic condition. (**C**) Results of incubation in ASW_HY supplemented with six different terminal electron acceptors for four (4D) or twelve (12D) days under anaerobic condition. (**D**) Results of incubation in ASW_HY supplemented with humic acid and Fe_2O_3 as the terminal electron acceptors for four days (4D) under anaerobic condition. (**E**) Results of incubation in ASW_Glucose (this contained 10 g L^{-1} D-glucose as the sole energy and carbon source) for four days (4D) under anaerobic condition. (**F**) Results of incubation in ASW_Pyruvate (this contained 5 g L^{-1} sodium pyruvate as the sole energy and carbon source) for four days (4D) under anaerobic condition. Final CFU counts recorded after the individual incubation periods have been plotted along the *y*-axes of the graphs, as the percentages of the corresponding initial CFU counts of the cultures (all initial and final CFU values underlying the six scatter plots are given in Table S1). All the percentage values shown here are arithmetic means of equivalent data obtained from three experimental replicates; standard deviation was < 2% of the mean for all the datasets in question. For all the percentage values in question, their Log_{10} transformations have been plotted to resolve the wide range of the values within a single frame. In each graph, the dotted grid line at the level of two 2 indicates the initial level (100%) of CFU count of the cultures concerned. The different isolates are placed along the *x*-axes of the individual graphs: **BreB**, *Brevibacterium* sp. BDJS002; **BreJ**, *Brevibacterium* sp. JSBI002; **Bru**, *Brucella anthropi* JSBI001; **Gor**, *Gordonia hongkongensis* SMJS1; **Hmo**, *Halomonas* sp. BDJS001; **Hps**, *Halopseudomonas bauzanensis* SMJS2; **Mar**, *Marinobacter segnicrescens* AN1; **Mes**, *Mesobacillus* sp. SBJS01; **Ste**, *Stenotrophomonas maltophilia* SBJS02.

Figure 2. Growth or survival of the OMZ-sediment isolates in ASW-based media supplemented with different complex carbon compounds, after incubations for four, eight, and four days, under aerobic, microaerobic, and anaerobic conditions, respectively. Results of incubation in ASW supplemented with (**A**) Type-I agar (2 g L^{-1}), (**B**) sodium alginate (10 g L^{-1}), (**C**) carrageenan (4 g L^{-1}), (**D**) chitosan (4 g L^{-1}), (**E**) sodium carboxymethylcellulose (5 g L^{-1}), (**F**) pectin (10 g L^{-1}), (**G**) xylan (10 g L^{-1}), (**H**) sodium benzoate (5 mM), and (**I**) starch (4 g L^{-1}), as the energy and carbon source, have been shown in the different panels. Final CFU counts recorded after the individual incubation periods have been plotted along the *y*-axes of the graphs, as the percentages of the corresponding initial CFU counts of the cultures (all initial and final CFU values underlying the different scatter plots are given in Table S2). All percentage values shown are arithmetic means of equivalent data obtained from three experimental

replicates; standard deviation was < 2% of the mean for all the datasets in question. For all percentage values, Log_{10} transformations have been plotted to resolve the wide range of the values. In each graph, the dotted grid line at the level of two 2 indicates the initial level (100%) of CFU count of the cultures. The different isolates are placed along the *x*-axes of the individual graphs: **BreB**, *Brevibacterium* sp. BDJS002; **BreJ**, *Brevibacterium* sp. JSBI002; **Bru**, *Brucella anthropi* JSBI001; **Gor**, *Gordonia hongkongensis* SMJS1; **Hmo**, *Halomonas* sp. BDJS001; **Hps**, *Halopseudomonas bauzanensis* SMJS2; **Mar**, *Marinobacter segnicrescens* AN1; **Mes**, *Mesobacillus* sp. SBJS01; **Ste**, *Stenotrophomonas maltophilia* SBJS02.

Figure 3. Growth or survival of the OMZ-sediment isolates in ASW-based media supplemented with extremely low concentration (1×10^{-12} g L^{-1}) of yeast extract (ASW_ELY) after incubations for four, eight, and four days, under aerobic, microaerobic, and anaerobic conditions, respectively. Results of incubation with (**A**) relatively higher (~10^6 cells mL^{-1} of culture) and (**B**) lower (~10^3 cells mL^{-1} of culture) initial cell density have been shown in the two panels. Final CFU counts recorded after the individual incubation periods have been plotted along the *y*-axes of the graphs, as the percentages of the corresponding initial CFU counts of the cultures (all initial and final CFU values underlying the two scatter plots are given in Table S3). All percentage values shown are arithmetic means of equivalent data obtained from three experimental replicates; standard deviation was < 2% of the mean for all the datasets in question. For all percentage values, Log_{10} transformations have been plotted to resolve the wide range of the values. In each graph, the dotted grid line at the level of two 2 indicates the initial level (100%) of CFU count of the cultures. The different isolates are placed along the *x*-axes of the individual graphs: **BreB**, *Brevibacterium* sp. BDJS002; **BreJ**, *Brevibacterium* sp. JSBI002; **Bru**, *Brucella anthropi* JSBI001; **Gor**, *Gordonia hongkongensis* SMJS1; **Hmo**, *Halomonas* sp. BDJS001; **Hps**, *Halopseudomonas bauzanensis* SMJS2; **Mar**, *Marinobacter segnicrescens* AN1; **Mes**, *Mesobacillus* sp. SBJS01; **Ste**, *Stenotrophomonas maltophilia* SBJS02.

Figure 4. Graphical representation of the annotated chromosomes of nine ASOMZ-sediment isolates. In each panel, the three concentric circles from the periphery to the center represent the following: size of the chromosome in megabases, distribution of CDSs along the positive strand, and distribution of CDSs along the negative strand; the pie diagram depicts the proportion at which the CDSs of the genome are distributed across the different COG categories. The same color code has been used to denote the different COG categories across the bars indicating CDSs in the two inner circles of each panel, and the pie diagrams drawn in the different panels. Names of the isolates for which the genomes were analyzed have been abbreviated as follows: **BreB**, *Brevibacterium* sp. BDJS002; **BreJ**, *Brevibacterium* sp. JSBI002; **Bru**, *Brucella anthropi* JSBI001; **Gor**, *Gordonia hongkongensis* SMJS1;

Hmo, *Halomonas* sp. BDJS001; **Hps**, *Halopseudomonas bauzanensis* SMJS2; **Mar**, *Marinobacter segnicrescens* AN1; **Mes**, *Mesobacillus* sp. SBJS01; **Ste**, *Stenotrophomonas maltophilia* SBJS02.

Figure 5. Graphical representation of the annotated plasmids of the three ASOMZ-sediment isolates *Brucella anthropi* JSBI001 (**Bru**), *Halopseudomonas bauzanensis* SMJS2 (**Hps**), and *Gordonia hongkongensis* SMJS1 (**Gor**). Names of the plasmids, as designated in the NCBI Genome database, are given in parentheses. In each panel, the three concentric circles from the periphery to the center represent (i) the size of the plasmid in kilobases, (ii) distribution of CDSs along the positive strand, and (iii) distribution of CDSs along the negative strand; the pie diagram depicts the proportion at which the CDSs of the plasmid are distributed across the different COG categories. The same color code has been used to denote the different COG categories across the bars indicating CDSs in the two inner circles of each panel, and the pie diagrams drawn in the different panels.

Figure 6. Heat map showing the distribution of all chromosome- and plasmid-borne CDSs of the ASOMZ-sediment isolates across the different COG categories: **BreB**, *Brevibacterium* sp. BDJS002; **BreJ**, *Brevibacterium* sp. JSBI002; **Bru**, *Brucella anthropi* JSBI001; **Gor**, *Gordonia hongkongensis* SMJS1; **Hmo**, *Halomonas* sp. BDJS001; **Hps**, *Halopseudomonas bauzanensis* SMJS2; **Mar**, *Marinobacter segnicrescens* AN1; **Mes**, *Mesobacillus* sp. SBJS01; **Ste**, *Stenotrophomonas maltophilia* SBJS02 (whether the CDS catalogs were from chromosomes or plasmids is indicated in parenthesis). For a given chromosome or plasmid, the percentage of its total CDSs ascribed to the different COG categories were first normalized by calculating the geometric means of the percentage values, and then dividing each percentage value by that mean (Table S7). Z-score normalization was performed upon the normalized CDS percentages across the individual chromosomes or plasmids. Z-scores were computed on a row by row basis by subtracting the mean of the normalized percentage values from each normalized percentage value and then dividing the individual remainders by the standard deviation of the normalized percentage values. As the rows were Z-Score scaled, cell colors represented how CDS percentages varied for a COG category across the chromosomes/plasmids, with white representing a row Z-Score of 0, while increasing positive and negative values are represented by the intensifying shades of blue and red respectively. The nine genomes and the four plasmids were further clustered in a dendogram (via Euclidean distance measurement) based on the Z-scores of their CDS distribution across the different COG categories.

Figure 7. Schematic diagram of different pathways of carbon metabolism encoded by the genomes of the OMZ-sediment isolates *Brevibacterium* sp. BDJS002 (**BreB**), *Brevibacterium* sp. JSBI002 (**BreJ**), *Brucella anthropi* JSBI001 (**Bru**), *Gordonia hongkongensis* SMJS1 (**Gor**), *Halomonas* sp. BDJS001 (**Hmo**), *Halopseudomonas bauzanensis* SMJS2 (**Hps**), *Marinobacter segnicrescens* AN1 (**Mar**),

Mesobacillus sp. SBJS01 (**Mes**), *Stenotrophomonas maltophilia* SBJS02 (**Ste**). The uppercase alphabetic codes assigned to the different biochemical transformations indicate different combinations of isolates that possess enzymes for the individual reactions: (**A**) BreB, BreJ, Bru, Gor, Hmo, Hps, Mar, Mes and Ste; (**B**) BreB, BreJ, Gor, Hmo, Hps, Mar, Mes and Ste; (**C**) BreB, BreJ, Bru, Gor, Hmo, Hps, Mes and Ste; (**D**) BreB, BreJ, Bru, Hmo, Hps, Mar and Mes; (**E**) BreB, BreJ, Bru, Gor, Hmo, Mes and Ste; (**F**) BreB, BreJ, Bru, Gor, Hmo and Hps; (**G**) BreB, BreJ, Bru, Hmo and Mar; (**H**) BreJ, Bru, Hmo, Hps and Mar; (**I**) Bru, Hmo, Hps, Mar and Mes; (**J**) BreB, Bru, Hmo and Hps; (**K**) BreB, Gor, Hmo and Hps; (**L**) BreB, Hmo and Hps; (**M**) Gor, Hmo and Hps; (**N**) BreB and BreJ; and (**O**) Hmo and Hps.

Figure 8. Histograms showing what percentages of the CDS contents of the different metagenomes assembled along (**A**) SSK42/5 and (**B**) SSK42/6 were ascribable to *Nitrosopumilus maritimus* and *Nitrosopumilus sediminis* on the basis of sequence similarity with homologous genes. The scales for both sediment-depth (plotted along the *y*-axes) and CDS percentage (plotted along the *x*-axes) are linear.

Table 1. Characteristic features of the chemoorganoheterotrophic bacterial strains isolated from Arabian Sea OMZ sediments

Phylum affiliation of the strains	Species-level identity of the strains	Total number of sibling strains isolated		Representative studied in details (source)	Isolation medium	Key metabolic attributes*	GenBank accession number	
		from SSK42/5	from SSK42/6				16S rRNA gene	Genome (plasmid, if any)
Actinobacteria	*Brevibacterium* sp.	1	3	BDJS002 = MCC 5171 (SSK42/6)	ASW_HY	OA, SF, EO, GAL, AA	OQ780597	CP116392
	Brevibacterium sp.	2	2	JSBI002 = MCC 5172 (SSK42/5)	ASW_HY	OA, SF, EO, GLUGAL, AA	OQ780604	CP110341
	Gordonia hongkongensis	2	1	SMJS1 (SSK42/5)	ASW_LY	OA, SF, EO, GLU, AA	OQ780429	CP123381 (CP123382, CP123383)
Firmicutes	*Mesobacillus* sp.	2	3	SBJS01 (SSK42/6)	ASW_HY	OA, SF, EO, GLUGAL	OQ780701	CP109811
Proteobacteria	*Brucella anthropi*	4	2	JSBI001 = MCC 5134 (SSK42/5)	ASW_HY	FA, SF, EO, GLUGAL, AA	OQ780596	CP110339 (CP110340)
	Halomonas sp.	2	4	BDJS001 = MCC 5128 (SSK42/6)	ASW_HY	OA, SF, EO, GLUGAL, AA	OQ780651	CP110535
	Halopseudomonas bauzanensis	1	1	SMJS2 (SSK42/5)	ASW_LY	FA, SF, EO, AA	OQ780586	CP123445 (CP123446)
	Marinobacter segnicrescens	1	3	AN1 = MCC 5129 (SSK42/6)	BBB_A	OA, SF, EO, GAL	OQ780700	CP110342
	Stenotrophomonas maltophilia	2	3	SBJS02 = MCC 5130 (SSK42/6)	ASW_HY	OA, SF, EO, GLUGAL	OQ780703	CP109812

* OA, obligately aerobic; FA, facultatively anaerobic (can grow via nitrate/nitrite reduction); SF, survival (partial maintenance of cell population) by fermentative metabolism; EO, extreme oligotrophy under aerobic and microaerobic conditions; GLU, growth on polyglucans (such as alginate, chitosan, starch and cellulose) under aerobic and microaerobic conditions; GAL, growth on polygalactans (such as agar, carrageenan and pectin) under aerobic and microaerobic conditions; GLUGAL, growth on polyglucans as well as polygalactans under aerobic and microaerobic conditions; AA, growth on aromatic compounds under aerobic condition only.

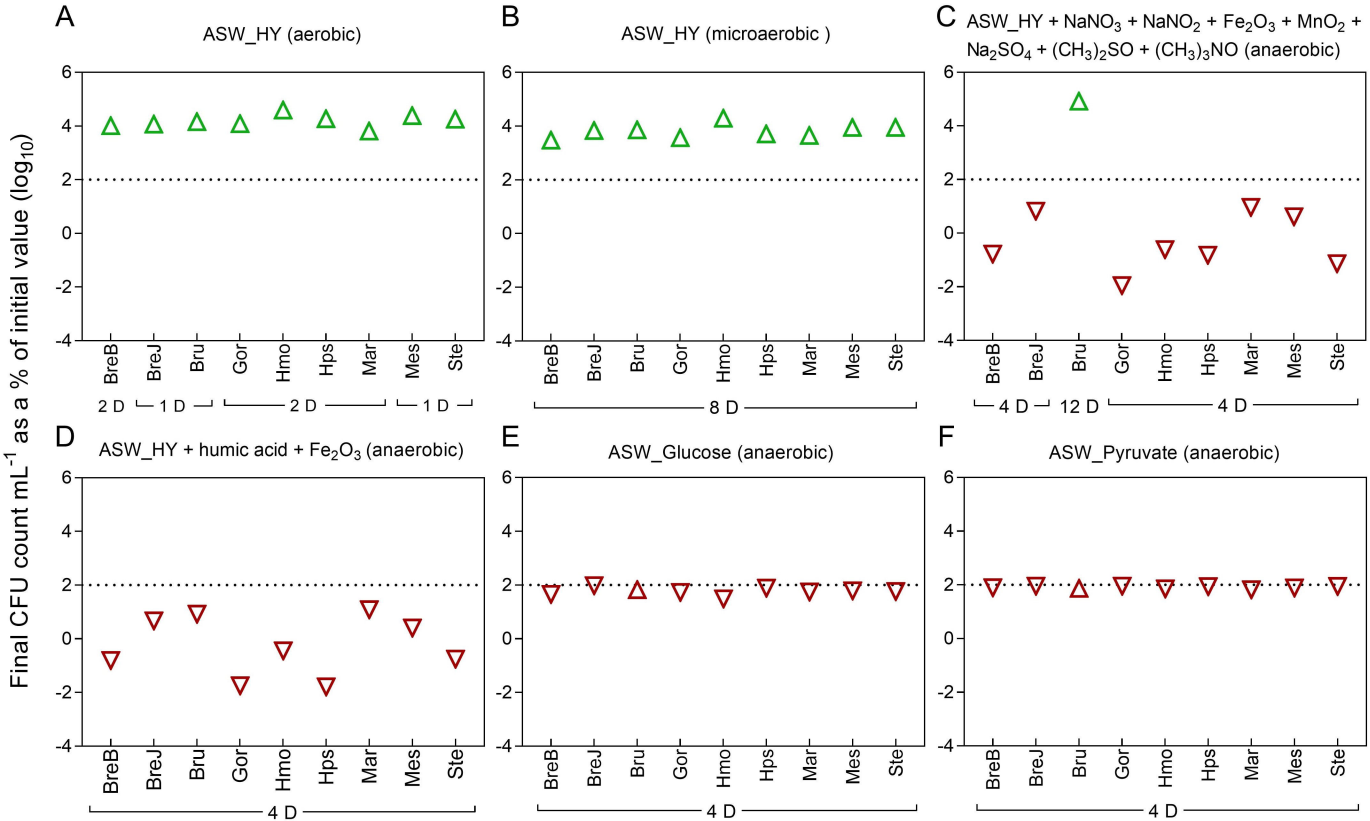
A
ASW_HY (aerobic)
B
ASW_HY (microaerobic)
C
ASW_HY + NaNO3 + NaNO2 + Fe2O3 + MnO2 + Na2SO4 + (CH3)2SO + (CH3)3NO (anaerobic)
D
ASW_HY + humic acid + Fe2O3 (anaerobic)
E
ASW_Glucose (anaerobic)
F
ASW_Pyruvate (anaerobic)
Final CFU count mL-1 as a % of initial value (log10)
6
4
2
0
-2
-4
BreB
BreJ
Bru
Gor
Hmo
Hps
Mar
Mes
Ste
2 D
1 D
2 D
1 D
8 D
4 D
12 D
4 D
4 D
4 D
4 D

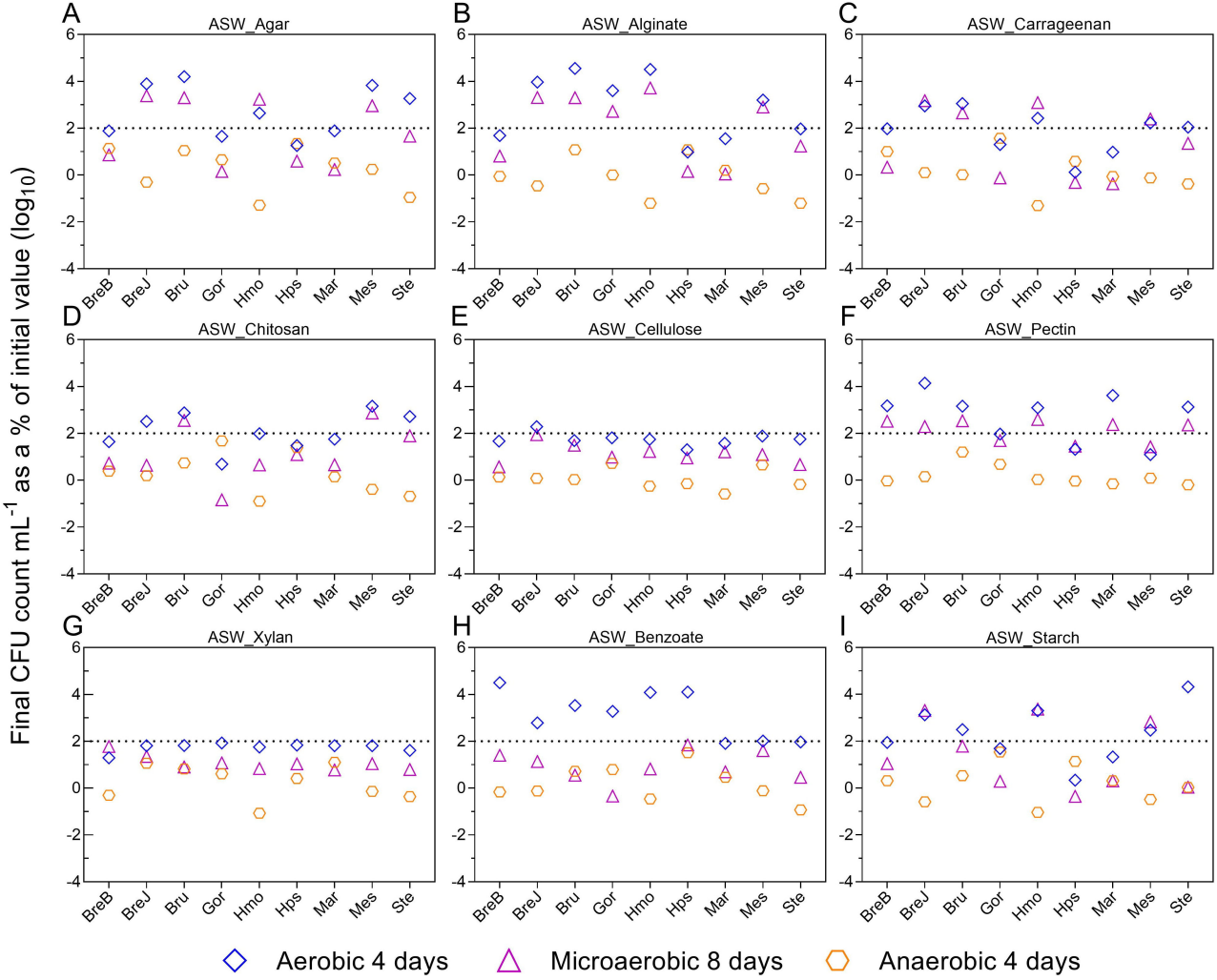
A
ASW_Agar
B
ASW_Alginate
C
ASW_Carrageenan
D
ASW_Chitosan
E
ASW_Cellulose
F
ASW_Pectin
G
ASW_Xylan
H
ASW_Benzoate
I
ASW_Starch
Final CFU count mL-1 as a % of initial value (log10)
6
4
2
0
-2
-4
BreB
BreJ
Bru
Gor
Hmo
Hps
Mar
Mes
Ste
Aerobic 4 days
Microaerobic 8 days
Anaerobic 4 days

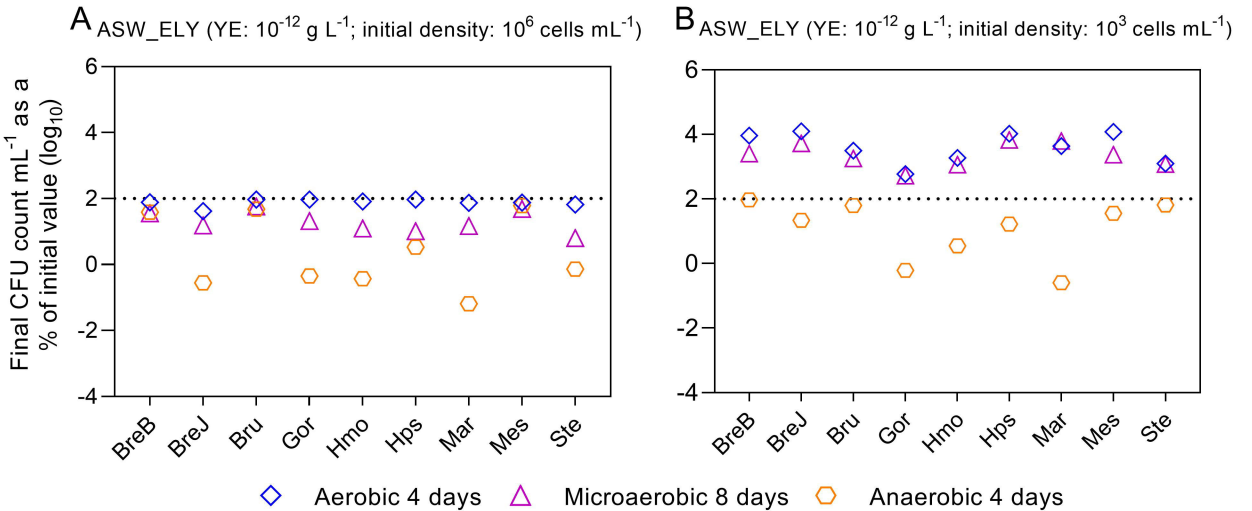
A ASW_ELY (YE: 10-12 g L-1; initial density: 106 cells mL-1)
B ASW_ELY (YE: 10-12 g L-1; initial density: 103 cells mL-1)
Final CFU count mL-1 as a % of initial value (log10)
6
4
2
0
-2
-4
BreB
BreJ
Bru
Gor
Hmo
Hps
Mar
Mes
Ste
Aerobic 4 days
Microaerobic 8 days
Anaerobic 4 days

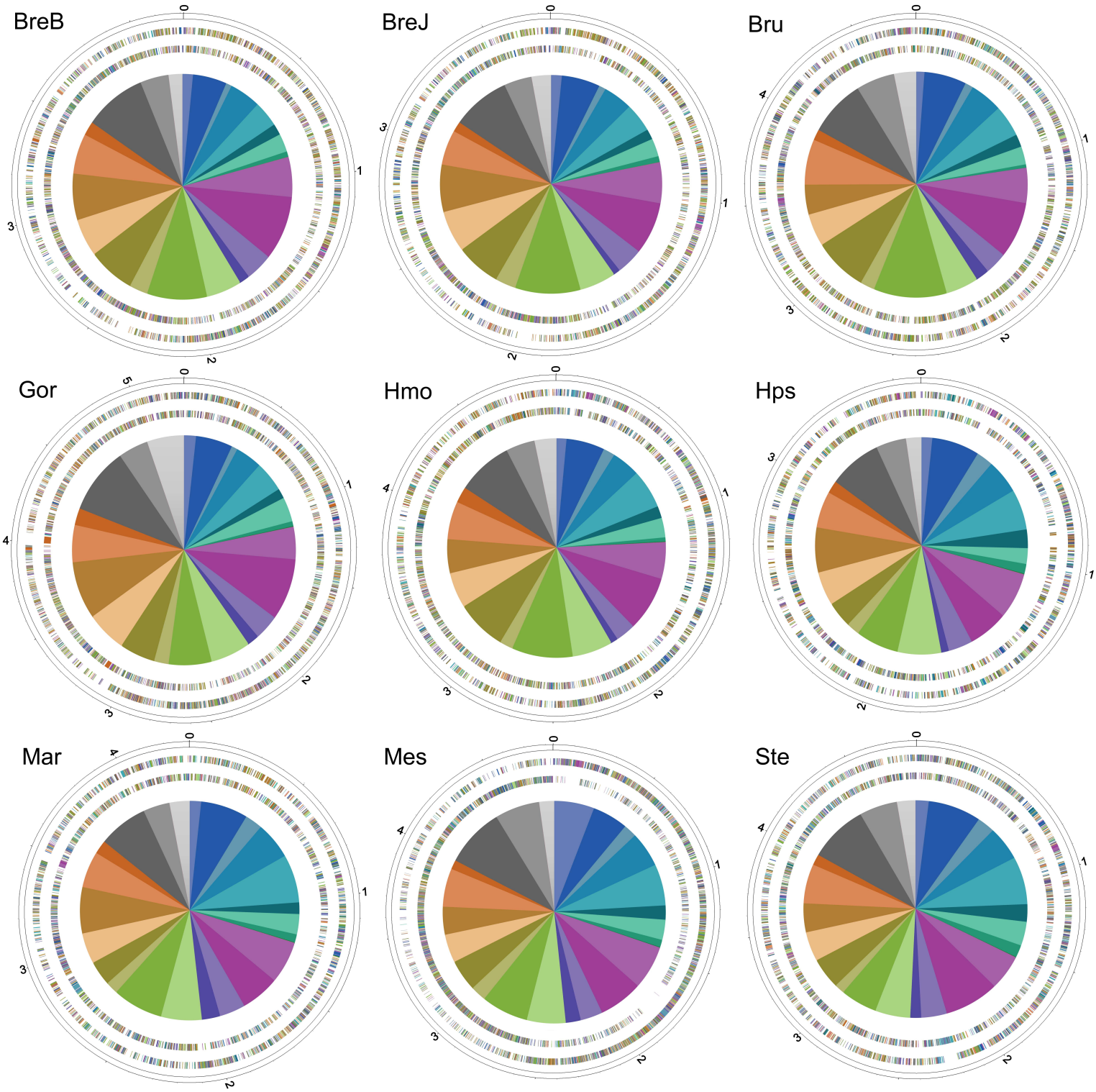

- Cell division and chromosome partitioning
- Cell wall structure and biogenesis and outer membrane
- Secretion, motility and chemotaxis
- Molecular chaperones and related functions
- Signal transduction
- Intracellular trafficking, secretion, and vesicular transport
- Defense mechanisms
- Extracellular structures
- Cell shape determination
- RNA processing and modification
- Translation, ribosomal structure and biogenesis
- Transcription
- Replication, recombination and repair
- Mobilome: prophages, transposons
- Energy production and conversion
- Amino acid transport and metabolism
- Nucleotide transport and metabolism
- Carbohydrate transport and metabolism
- Coenzyme transport and metabolism
- Lipid transport and metabolism
- Inorganic ion transport and metabolism
- Secondary metabolites biosynthesis, transport and catabolism
- General function prediction only
- Function unknown

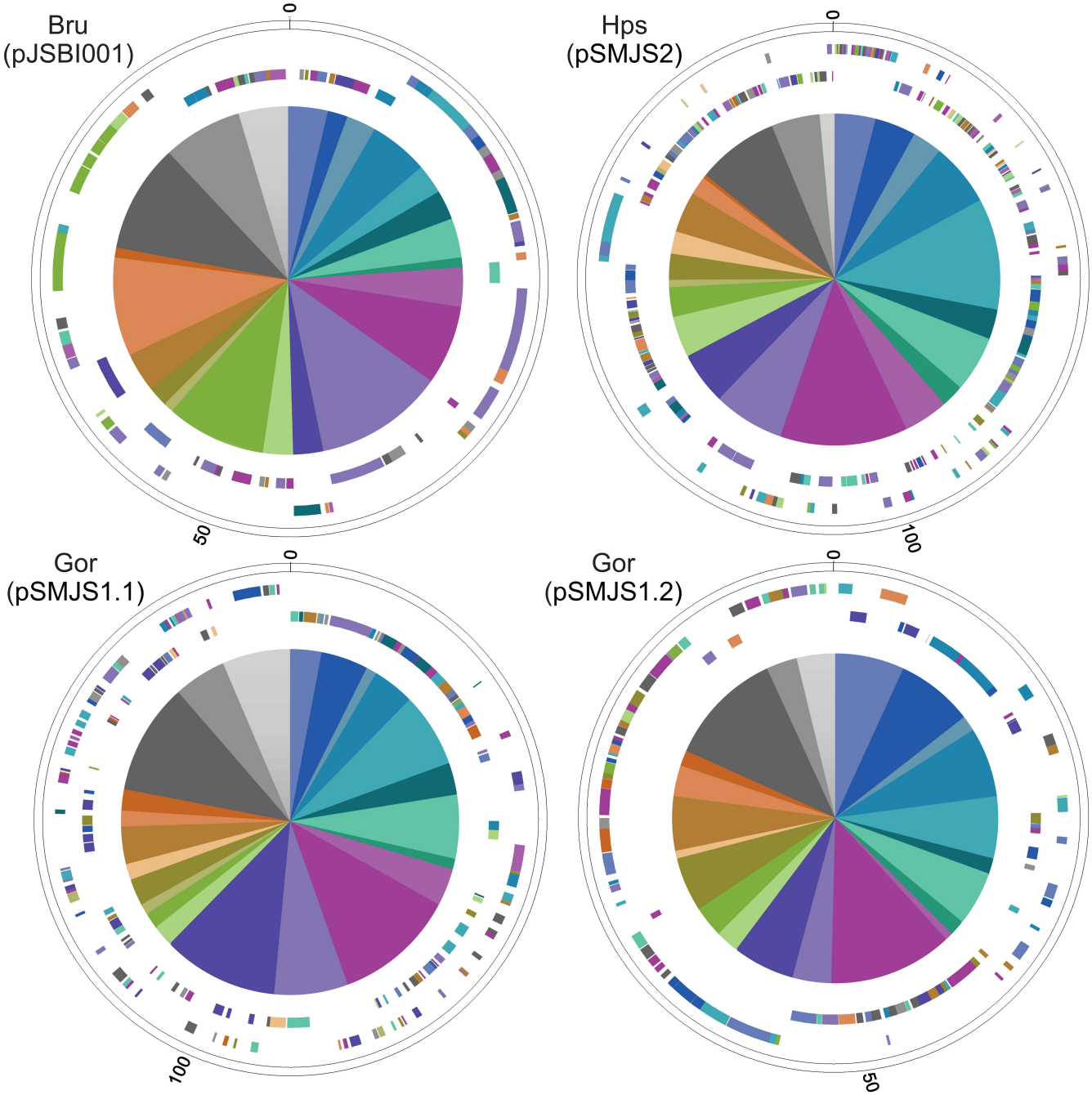

- Cell division and chromosome partitioning
- Cell wall structure and biogenesis and outer membrane
- Secretion, motility and chemotaxis
- Molecular chaperones and related functions
- Signal transduction
- Intracellular trafficking, secretion, and vesicular transport
- Defense mechanisms
- Extracellular structures
- Cell shape determination
- RNA processing and modification
- Translation, ribosomal structure and biogenesis
- Transcription
- Replication, recombination and repair
- Mobilome: prophages, transposons
- Energy production and conversion
- Amino acid transport and metabolism
- Nucleotide transport and metabolism
- Carbohydrate transport and metabolism
- Coenzyme transport and metabolism
- Lipid transport and metabolism
- Inorganic ion transport and metabolism
- Secondary metabolites biosynthesis, transport and catabolism
- General function prediction only
- Function unknown

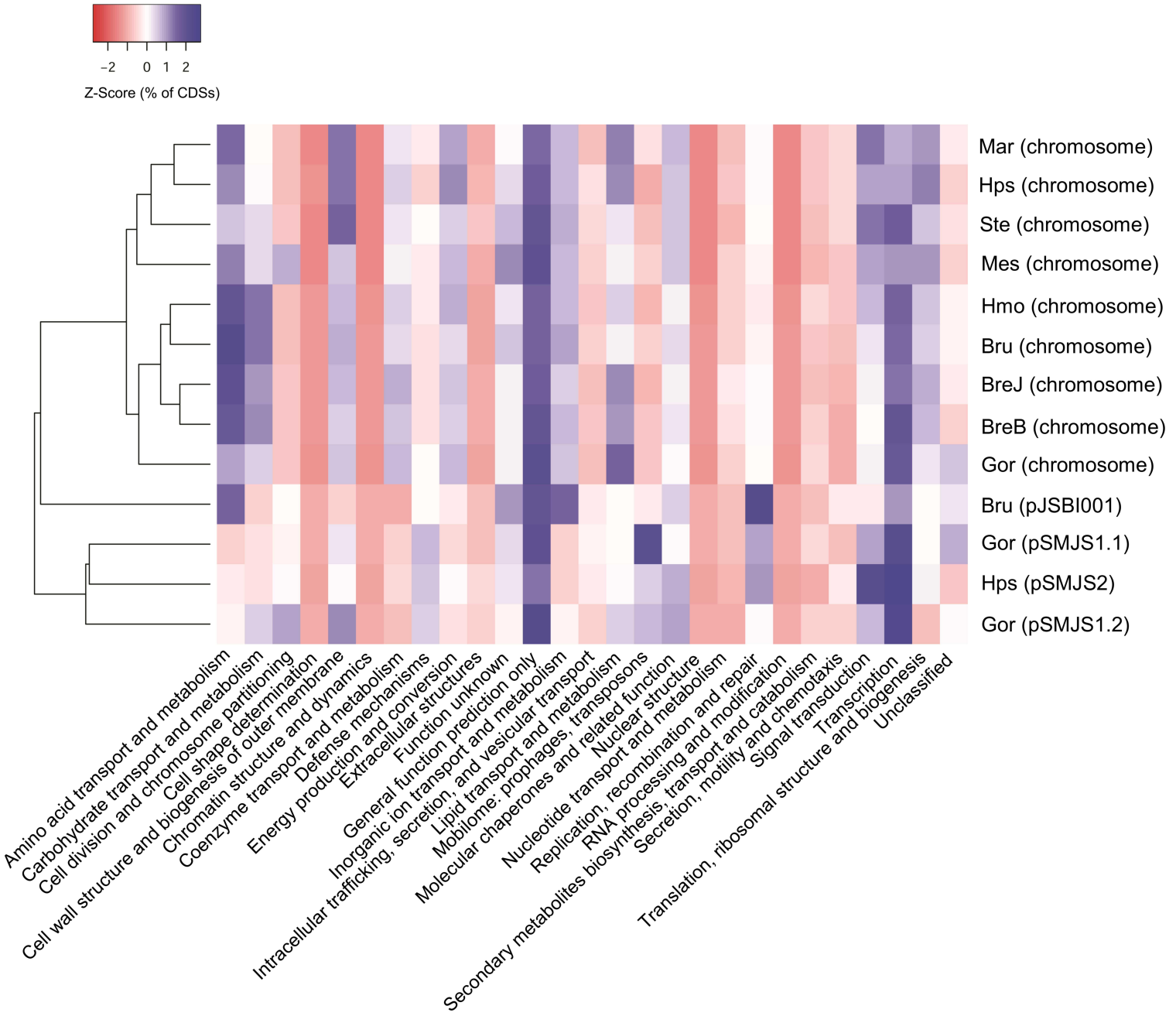
−2
0
1
2
Z-Score (% of CDSs)
Mar (chromosome)
Hps (chromosome)
Ste (chromosome)
Mes (chromosome)
Hmo (chromosome)
Bru (chromosome)
BreJ (chromosome)
BreB (chromosome)
Gor (chromosome)
Bru (pJSBI001)
Gor (pSMJS1.1)
Hps (pSMJS2)
Gor (pSMJS1.2)
Amino acid transport and metabolism
Carbohydrate transport and metabolism
Cell division and chromosome partitioning
Cell shape determination
Cell wall structure and biogenesis of outer membrane
Chromatin structure and dynamics
Coenzyme transport and metabolism
Defense mechanisms
Energy production and conversion
Extracellular structures
Function unknown
General function prediction only
Inorganic ion transport and metabolism
Intracellular trafficking, secretion, and vesicular transport
Lipid transport and metabolism
Mobilome: prophages, transposons
Molecular chaperones and related function
Nuclear structure
Nucleotide transport and metabolism
Replication, recombination and repair
RNA processing and modification
Secondary metabolites biosynthesis, transport and catabolism
Secretion, motility and chemotaxis
Signal transduction
Transcription
Translation, ribosomal structure and biogenesis
Unclassified

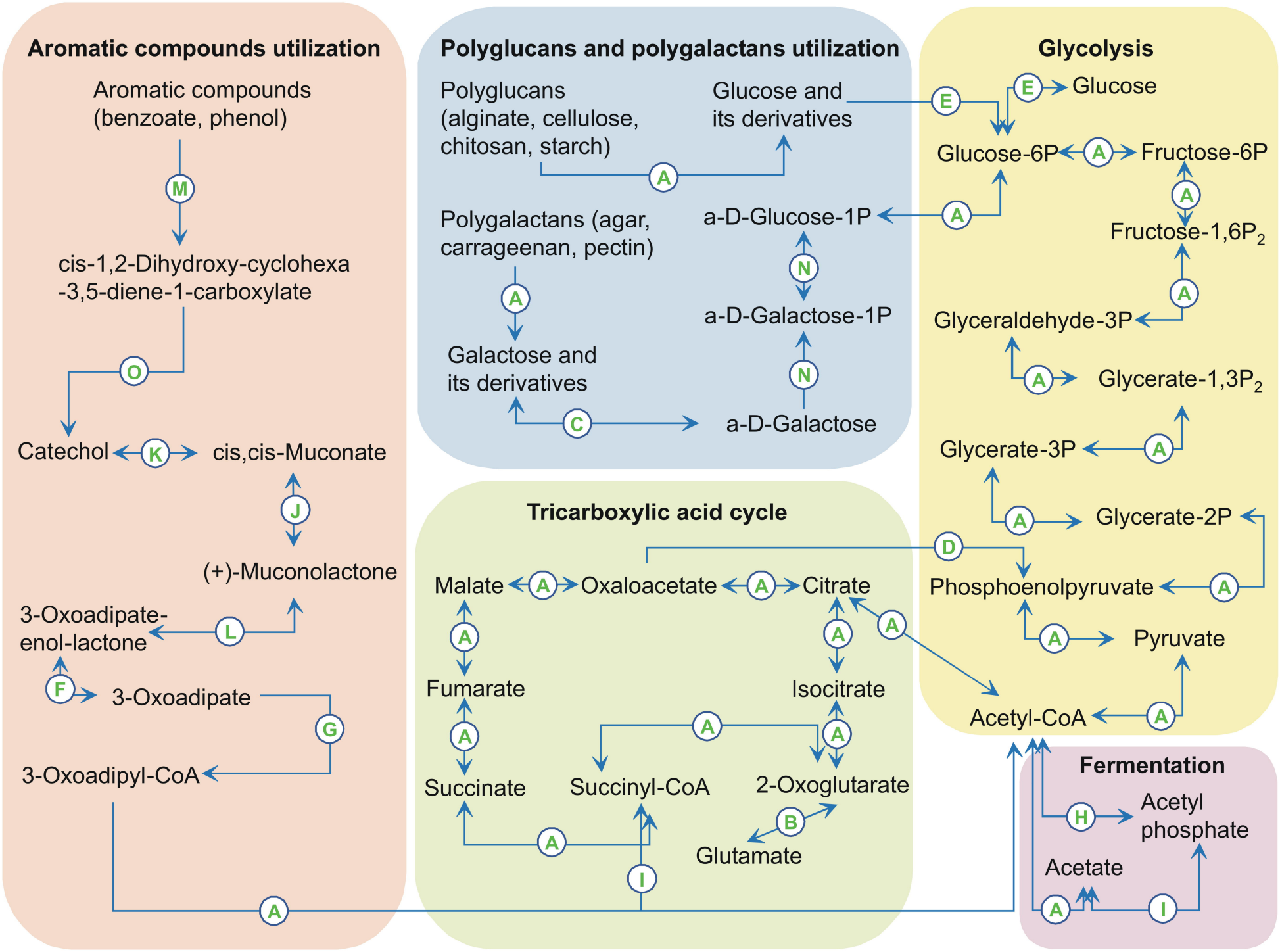
Aromatic compounds utilization
Aromatic compounds (benzoate, phenol)
M
cis-1,2-Dihydroxy-cyclohexa -3,5-diene-1-carboxylate
O
Catechol
K
cis,cis-Muconate
J
(+)-Muconolactone
3-Oxoadipate-enol-lactone
L
F
3-Oxoadipate
G
3-Oxoadipyl-CoA
A
Polyglucans and polygalactans utilization
Polyglucans (alginate, cellulose, chitosan, starch)
Glucose and its derivatives
A
Polygalactans (agar, carrageenan, pectin)
a-D-Glucose-1P
N
A
a-D-Galactose-1P
Galactose and its derivatives
N
C
a-D-Galactose
Glycolysis
E
E
Glucose
Glucose-6P
A
Fructose-6P
A
A
Fructose-1,6P2
A
Glyceraldehyde-3P
A
Glycerate-1,3P2
Glycerate-3P
A
A
Glycerate-2P
D
Phosphoenolpyruvate
A
A
Pyruvate
Acetyl-CoA
A
Tricarboxylic acid cycle
Malate
A
Oxaloacetate
A
Citrate
A
A
A
Fumarate
Isocitrate
A
A
A
Succinate
Succinyl-CoA
2-Oxoglutarate
B
A
Glutamate
I
Fermentation
H
Acetyl phosphate
Acetate
A
I

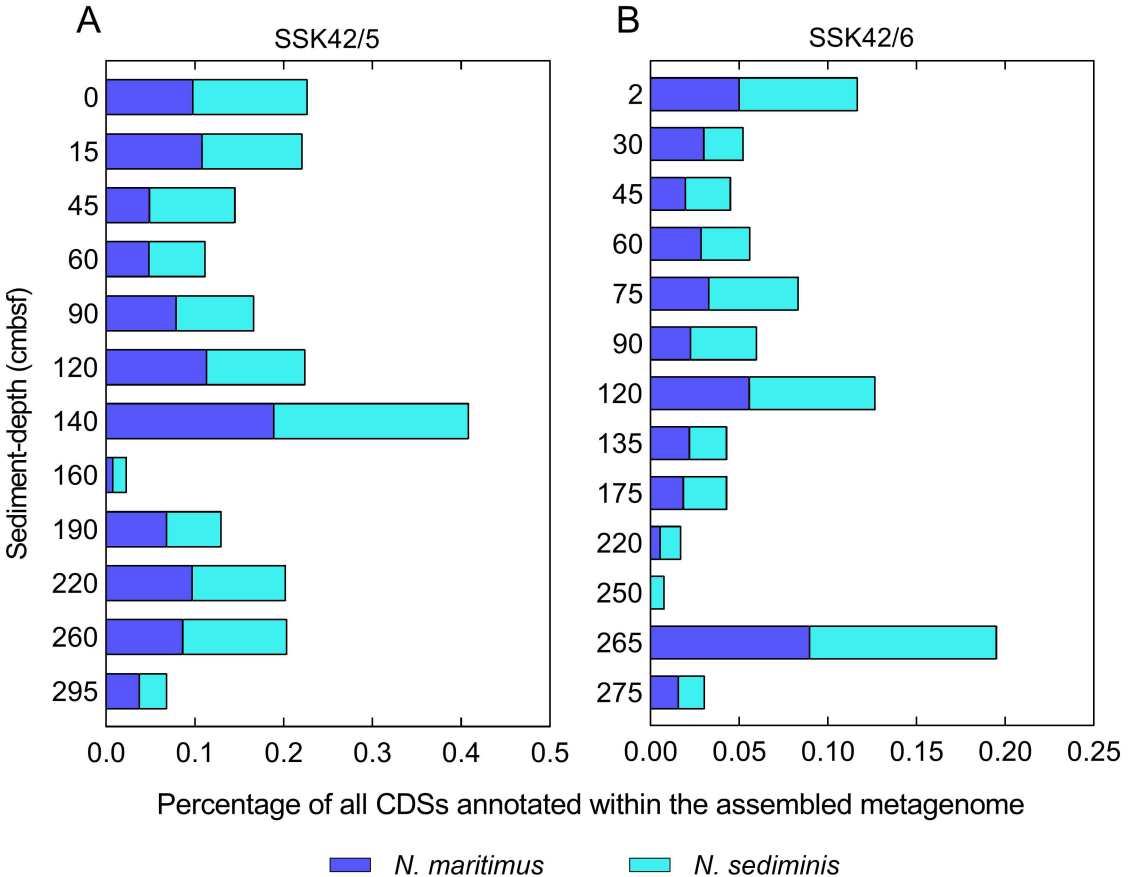
A
SSK42/5
B
SSK42/6
Sediment-depth (cmbsf)
0
15
45
60
90
120
140
160
190
220
260
295
2
30
45
60
75
90
120
135
175
220
250
265
275
0.0
0.1
0.2
0.3
0.4
0.5
0.00
0.05
0.10
0.15
0.20
0.25
Percentage of all CDSs annotated within the assembled metagenome
N. maritimus
N. sediminis